

Synthesis and properties of novel energetic (cyano-*NNO*-azoxy)furazans

**Nikita E. Leonov, Fedor M. Sidorov, Michael S. Klenov, Aleksandr M. Churakov,
Yurii A. Strelenko, Alla N. Pivkina, Ivan V. Fedyanin, David B. Lempert,
Tatiana S. Kon'kova, Yurii N. Matyushin and Vladimir A. Tartakovsky**

Contents

Experimental Section	S2
¹ H NMR (600.1 MHz, [D ₆]acetone) of compound 3	S5
¹³ C NMR (150.9 MHz, [D ₆]acetone) of compound 3	S6
¹⁴ N NMR (43.4 MHz, [D ₆]acetone) of compound 3	S7
¹⁵ N NMR ([INVGATED], 60.8 MHz, [D ₆]acetone) of compound 3	S8
IR of compound 3	S9
HRMS of compound 3	S10
¹³ C NMR (125.8 MHz, [D ₆]acetone) spectrum of compound 4	S11
¹⁴ N NMR (43.4 MHz, [D ₆]acetone) spectrum of compound 4	S12
¹⁵ N NMR ([INVGATED], 60.8 MHz, [D ₆]acetone) of compound 4	S13
IR of compound 4	S14
HRMS of compound 4	S15
¹ H NMR (600.1 MHz, [D ₆]acetone) spectrum of compound 6	S16
¹³ C NMR (150.9 MHz, [D ₆]acetone) spectrum of compound 6	S17
¹⁴ N NMR (43.4 MHz, [D ₆]acetone) of compound 6	S18
¹⁵ N NMR ([INVGATED], 60.8 MHz, [D ₆]acetone) of compound 6	S19
IR of compound 6	S20
HRMS of compound 6	S21
X-ray crystal structure determination	S22
DSC of compound 3	S27
DSC of compound 4	S28
DSC of compound 6	S29
Calorimetric measurements	S30
Combustion performance	S35

Experimental Section

Safety precautions

While we have experienced no difficulties in synthesis and characterization of these energetic materials, proper protective measures should be used. Manipulations must be carried out in a hood behind a safety shield. Face shield and leather gloves must be worn. Mechanical actions involving scratching or scraping must be avoided.

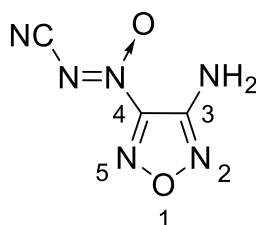
General Remarks: ^1H , ^{13}C , ^{14}N and ^{15}N NMR spectra were recorded with Bruker DRX-500 (500.1, 125.8, 36.1, 50.7 MHz, respectively) and Bruker AV600 (600.1, 150.9, 43.4, 60.8 MHz, respectively) spectrometers. Chemical shifts are reported in delta (δ) units, parts per million (ppm) downfield from internal TMS (^1H , ^{13}C) or external CH_3NO_2 (^{14}N , ^{15}N negative values of δ_{N} correspond to upfield shifts). The IR spectra were recorded with a Bruker ALPHA-T spectrometer in the range 400–4000 cm^{-1} (resolution 2 cm^{-1}) as pellets with KBr. High-resolution ESI mass spectra (HRMS) were recorded with a Bruker micrOTOF II instrument. Melting points were determined with a Kofler melting point apparatus and are uncorrected. Thermal behavior was studied using Netzsch DSC 204 HP in nitrogen flow. A sample of ca. 0.5 mg was placed in closed aluminum crucibles with pierced lids and heated linearly at 5 $\text{K}\cdot\text{min}^{-1}$ rate up to 400 $^{\circ}\text{C}$. The impact and friction sensitivities of compounds **3**, **4** and **6** were determined using a STANAG protocol and BAM-type impact and friction machines.^{1,2} Silica gel 60 Merck (15–40 μm) was used for preparative column and thin-layer chromatography. Silica gel “Silpearl UV 254” was used for preparative column and thin-layer chromatography. Analytical thin-layer chromatography (TLC) was carried out on Merck silica gel 60 F254 and “Silufol” TLC silica gel UV-254 aluminum sheets. *Solvents were purified* before use, according to standard procedures. All other reagents were used without further purification. 2,2,2-Trifluoro-*N*-(4-nitrosfurazan-3-yl)acetamide (**1**) was prepared according to the reported procedure.³

¹ STANAG 4489, Explosives, Impact Sensitivity Tests, 1st ed., NATO standardization agreement, NATO, Brussels (Belgium), 1999.

² STANAG 4487, Explosives, Friction Sensitivity Tests, 1st ed., NATO standardization agreement, NATO, Brussels (Belgium), 2002.

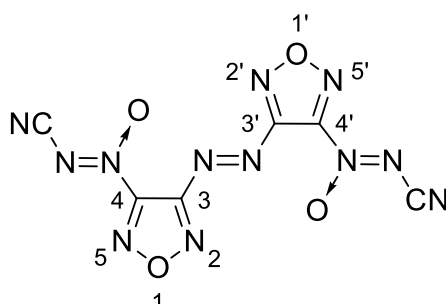
³ N. E. Leonov, M. S. Klenov, O. V. Anikin, A. M. Churakov, Yu. A. Strelenko, A. A. Voronin, D. B. Lempert, N. V. Muravyev, I. V. Fedyanin, S. E. Semenov and V. A. Tartakovsky, *ChemistrySelect*, 2020, **5**, 12243.

3-Amino-4-(2-cyano-1-oxidodiazenyl)furazan 3. A solution of cyanamide (400 mg, 9.52 mmol) in dry ether (20 ml) was added dropwise to a stirred suspension of 2,2,2-trifluoro-*N*-(4-nitrosfurazan-3-yl)acetamide **1** (2.0 g, 9.52 mmol) and DBI (2.73 g, 9.52 mmol) in dry CH₂Cl₂ (60 ml) at 0 °C under argon. The mixture was warmed to 25 °C and vigorously stirred at this temperature for 24 h. The precipitate was then filtered off, washed with CH₂Cl₂ (2 × 50 ml). The combined filtrates were concentrated under reduced pressure. The residue was dissolved in MeOH (16 ml), and the solution of CF₃CO₂H (0.2 ml) in H₂O (6 ml) was added. The resulting reaction mixture was kept at –20 °C for 24 h. Then it was concentrated under reduced pressure and the residue was purified by flash chromatography (petroleum ether/ethyl acetate, 5 : 1, R_f (**3**) = 0.19). The combined eluates were concentrated under reduced pressure at 35 °C to ~50 ml volume. The resulting precipitate was collected by filtration, washed with cold hexane (2 × 25 ml) and dried in air to give furazan **3** (0.98 g, 67%) as a yellow solid, m.p.: 117–118 °C. DSC (5 °C·min⁻¹): T_m = 117 °C, T_{onset} = 209 °C (dec.).



¹H NMR (600.1 MHz, [D₆]acetone): δ = 6.65 (br. s, 2 H, NH₂) ppm. ¹³C NMR (150.9 MHz, [D₆]acetone): δ = 109.8 (CN), 152.0 (br., C-4), 152.1 (C-3) ppm. ¹⁴N NMR (43.4 MHz, [D₆]acetone): δ = –43 (N(O)=N–CN, Δv_{1/2} = 50 Hz), –118 (N(O)=N–CN, Δv_{1/2} = 880 Hz), –340 (NH₂, Δv_{1/2} = 800 Hz). ¹⁵N NMR ([INVGATED], 60.8 MHz, [D₆]acetone): δ = 35.0, 2.3 (furazan ring), –42.3 (N(O)=N–CN), –99.4 (N(O)=N–CN), –117.6 (N(O)=N–CN), –335.6 (NH₂). IR (KBr): ν = 3463 (s), 3361 (s), 3211 (w), 3158 (w), 2208 (w), 1635 (s), 1584 (m), 1500 (m), 1453 (s), 1420 (m), 1359 (s), 1218 (m) cm⁻¹. HRMS (ESI): *m/z* calcd for C₃H₂N₆O₂ [M + Ag]⁺ 260.9285; found 260.9288. Anal. calcd for C₃H₂N₆O₂: C 23.38, H 1.31, N 54.54, found: C 23.41, H 1.35, N 54.44.

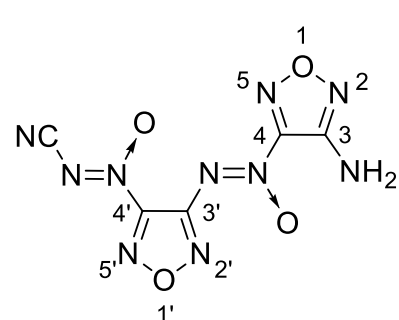
4,4'-Bis(2-cyano-1-oxidodiazenyl)-3,3'-azofurazan 4. Finely powdered DBI (8.71 g, 30.37 mmol) was added portionwise to a stirred suspension of compound **3** (2.34 g, 15.19 mmol) in dry CH₂Cl₂ (45 ml) at 25 °C under argon. The mixture was vigorously stirred at this temperature for 24 h. The precipitate was then filtered off, washed with CH₂Cl₂ (4 × 50 ml). The combined filtrates were concentrated under reduced pressure, and the residue was purified by preparative column chromatography (petroleum ether/ethyl acetate, 5 : 1, containing 0.5% v/v of trifluoroacetic acid, R_f (**4**) = 0.49) to give product **4** (1.61 g, 70%) as an orange solid, m.p.: 90–91 °C. DSC (5 °C·min⁻¹): T_m = 90 °C, T_{onset} = 222 °C (dec.).



¹³C NMR (125.8 MHz, [D₆]acetone): δ = 109.5 (CN), 155.2 (br., C-4 & C-4'), 157.9 (C-3 & C-3') ppm. ¹⁴N NMR (43.4 MHz, [D₆]acetone): δ = 147 (N=N, Δv_{1/2} = 1000 Hz), –49 (N(O)=N–CN, Δv_{1/2} = 40 Hz), –114 (N(O)=N–CN, Δv_{1/2} = 750 Hz). ¹⁵N NMR ([INVGATED], 60.8 MHz, [D₆]acetone): δ = 145.5 (N=N), 40.7, 34.7 (furazan rings), –48.7

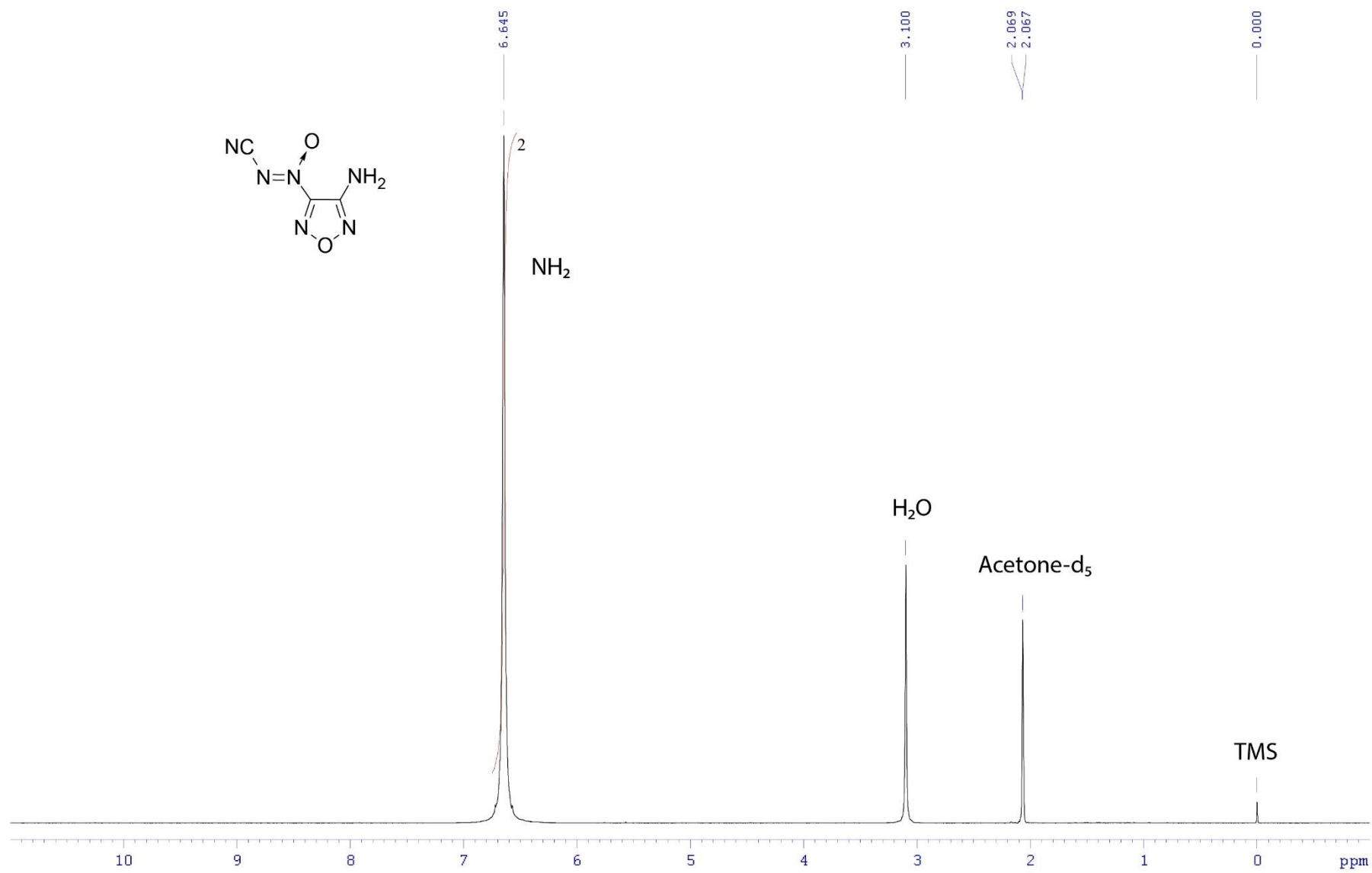
(N(O)=N–CN), –87.2 (N(O)=N–CN), –112.3 (N(O)=N–CN). IR (KBr): ν = 2203 (w), 1559 (w), 1492 (s), 1419 (w), 1333 (w), 1198 (m) cm^{-1} . HRMS (ESI): m/z calcd for $\text{C}_6\text{N}_{12}\text{O}_4$ [$\text{M} + \text{Na}$] $^+$ 327.0058; found 327.0060. Anal. calcd for $\text{C}_6\text{N}_{12}\text{O}_4$: C 23.69, N 55.26, found: C 23.71, N 55.15.

3-Amino-4-{2-[4-(2-cyano-1-oxidodiazenyl)furazan-3-yl]-1-oxidodiazenyl}furazan 6. Compound **3** (2.0 g, 12.98 mmol) was added portionwise to a stirred suspension of compound **1** (5.5 g, 26.18 mmol) and DBI (7.51 g, 26.18 mmol) in a mixture of MeCN (10 ml) and CH_2Cl_2 (10 ml) at 0 °C under argon. The mixture was warmed to 25 °C and vigorously stirred at this temperature for 24 h. The precipitate was then filtered off and washed with CH_2Cl_2 (3×50 ml). The combined filtrates were concentrated under reduced pressure. The residue was dissolved in MeOH (40 ml), and a solution of $\text{CF}_3\text{CO}_2\text{H}$ (1 ml) in H_2O (30 ml) was added. The resulting mixture was kept at –20 °C for 24 h. Then it was concentrated under reduced pressure, and the residue was purified by flash chromatography (petroleum ether/ethyl acetate, 5 : 1, containing 0.5% v/v of trifluoroacetic acid, R_f (**6**) = 0.18). The combined eluates were concentrated under reduced pressure to a volume of ~50 ml. The resulting precipitate was collected by filtration, washed with cold hexane (2×25 ml) and dried in air to give product **6** (2.14 g, 62%) as a yellow solid, m.p.: 124–125 °C. DSC ($5 \text{ }^\circ\text{C} \cdot \text{min}^{-1}$): T_m = 124 °C, T_{onset} = 193 °C (dec.).

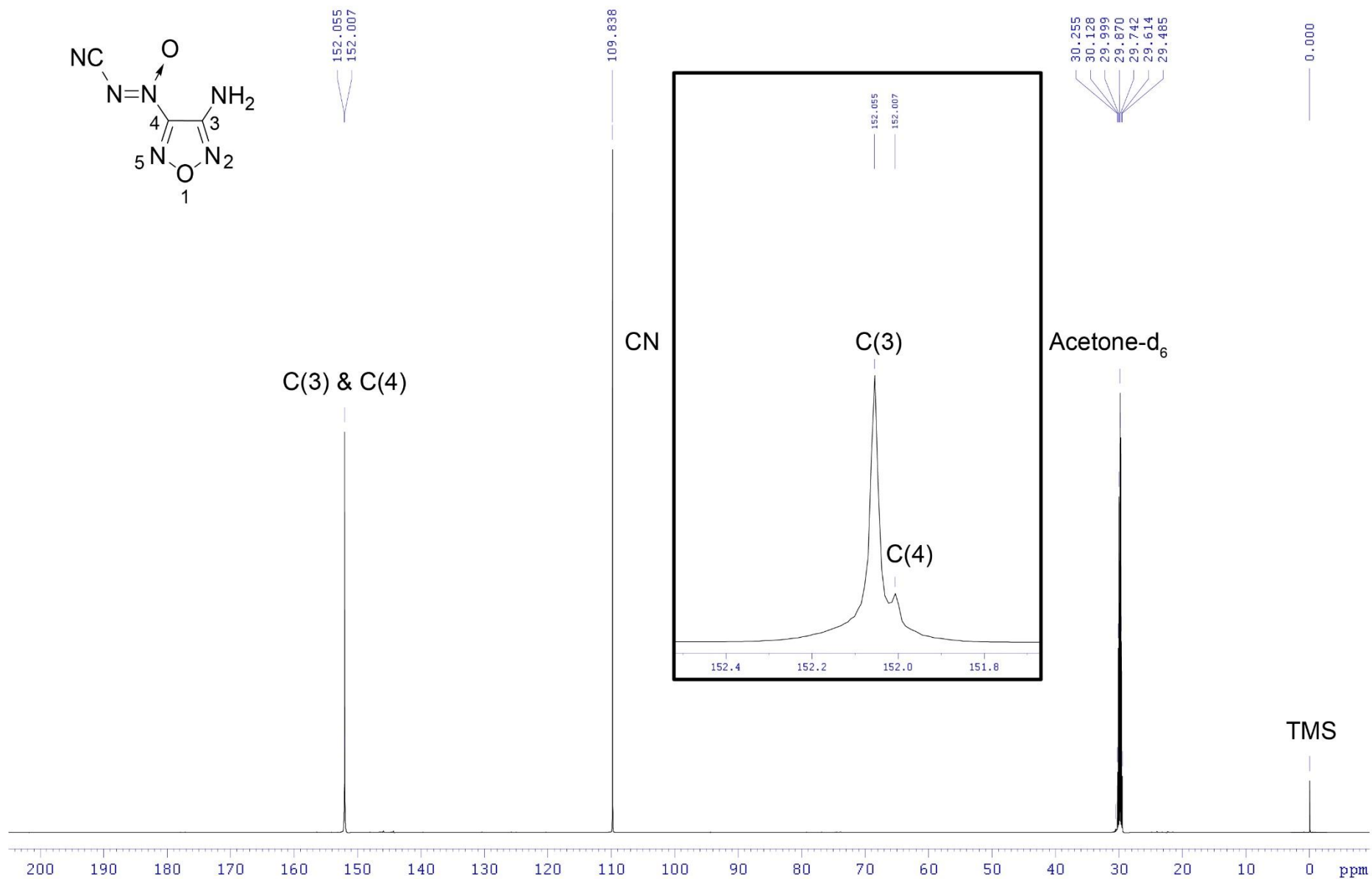


^1H NMR (600.1 MHz, $[\text{D}_6]$ acetone): δ = 6.69 (br. s, 2 H, NH_2) ppm. ^{13}C NMR (150.9 MHz, $[\text{D}_6]$ acetone): δ = 109.7 (CN), 149.6 (C-3 or C-3'), 151.9 (C-3 or C-3'), 153.0 (br., C-4 or C-4'), 155.6 (br., C-4 or C-4') ppm. ^{14}N NMR (43.4 MHz, $[\text{D}_6]$ acetone): δ = –48 (N(O)=N–CN, $\Delta v_{1/2}$ = 55 Hz), –59 (Fz–N(O)=N–Fz, $\Delta v_{1/2}$ = 75 Hz), –114 (N(O)=N–CN, $\Delta v_{1/2}$ = 900 Hz), –345 (NH_2 , $\Delta v_{1/2}$ = 1200 Hz). ^{15}N NMR ([INVGATED], 60.8 MHz, $[\text{D}_6]$ acetone): δ = 38.7, 35.7, 33.9, 1.4 (furazan rings), –47.1 (N(O)=N–CN), –58.8 (Fz–N(O)=N–Fz), –87.2, –89.4 (Fz–N(O)=N–Fz and N(O)=N–CN), –113.4 (N(O)=N–CN), –336.4 (NH_2). IR (KBr): ν = 3467 (s), 3336 (s), 3251 (w), 3187 (w), 2203 (w), 2191 (w), 1630 (s), 1564 (w), 1541 (m), 1507 (s), 1489 (s), 1451 (m), 1430 (m), 1402 (m), 1357 (m), 1330 (m), 1221 (m), 1169 (m), 1109 (w) cm^{-1} . HRMS (ESI): m/z calcd for $\text{C}_5\text{H}_2\text{N}_{10}\text{O}_4$ [$\text{M} + \text{H}$] $^+$ 269.0490; found 269.0488. Anal. calcd for $\text{C}_5\text{H}_2\text{N}_{10}\text{O}_4$: C 22.57, H 0.76, N 52.63, found: C 22.61, H 0.77, N 52.50.

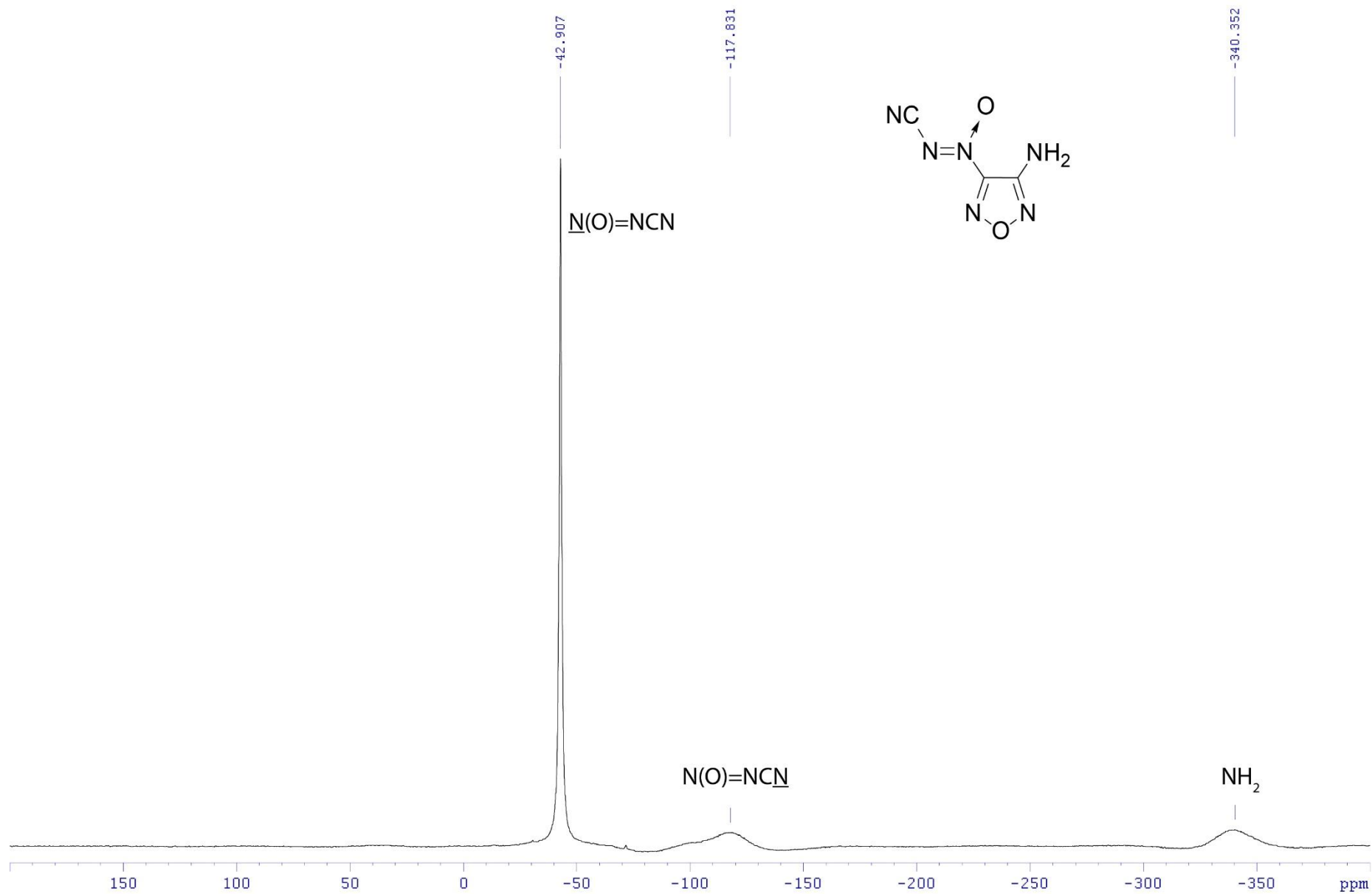
¹H NMR (600.1 MHz, [D₆]acetone) of compound 3



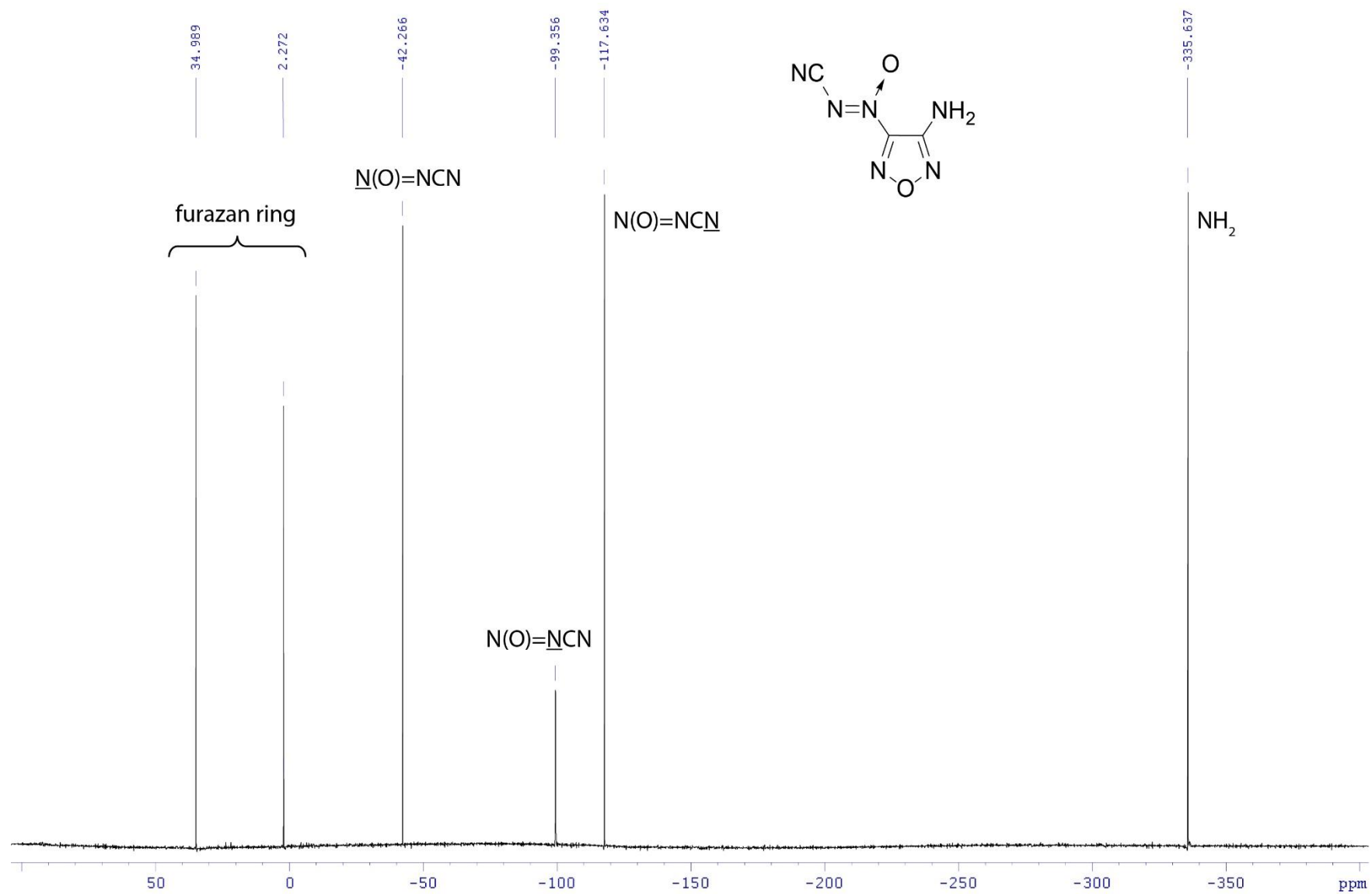
¹³C NMR (150.9 MHz, [D₆]acetone) of compound 3



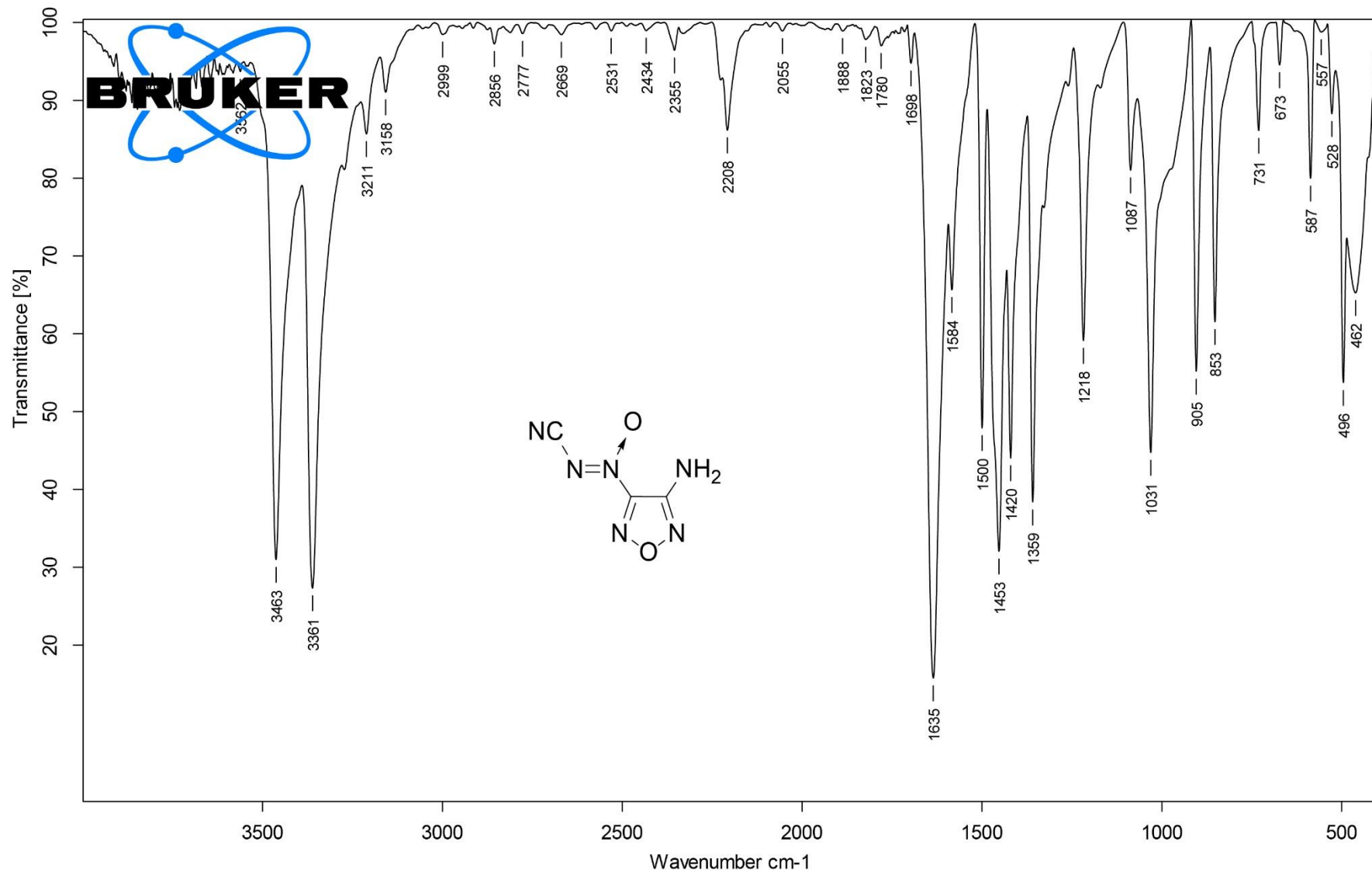
¹⁴N NMR (43.4 MHz, [D₆]acetone) of compound 3



¹⁵N NMR ([INVGATED], 60.8 MHz, [D₆]acetone) of compound 3



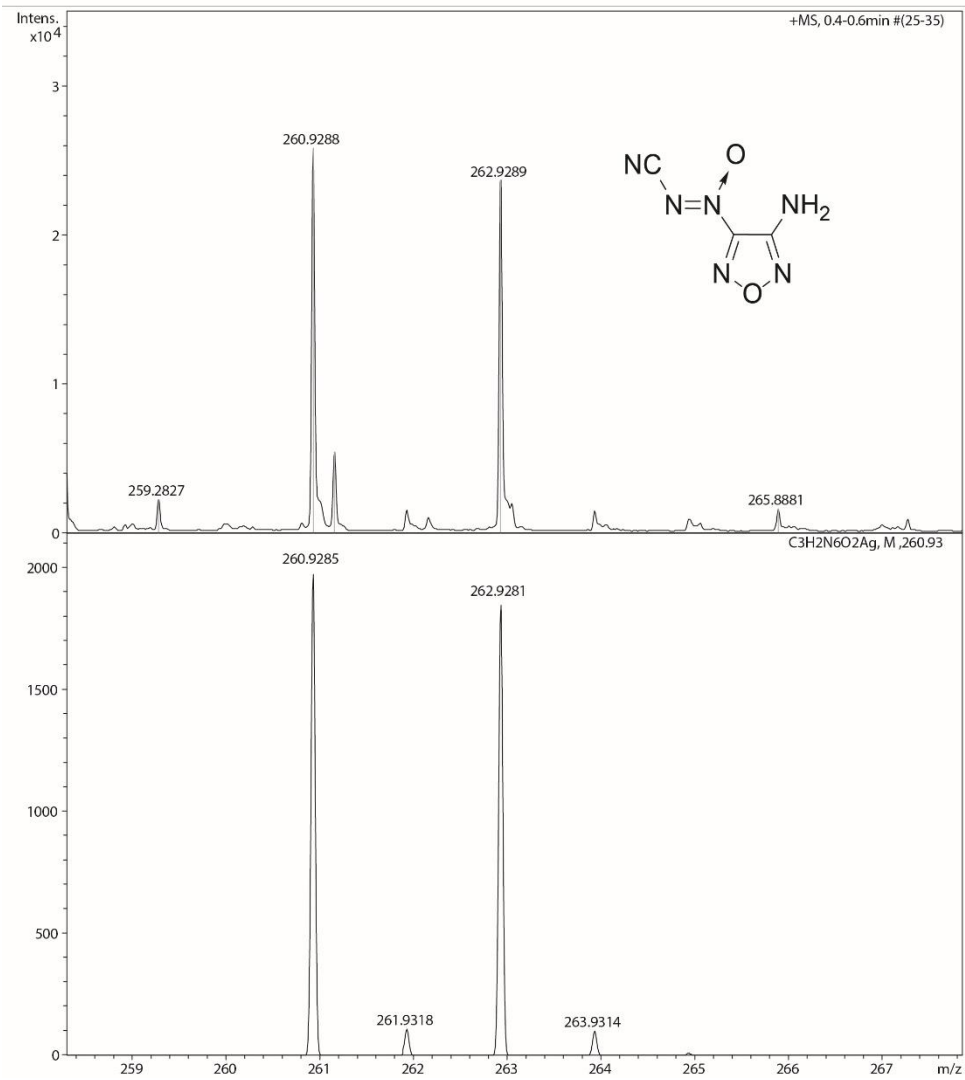
IR of compound 3



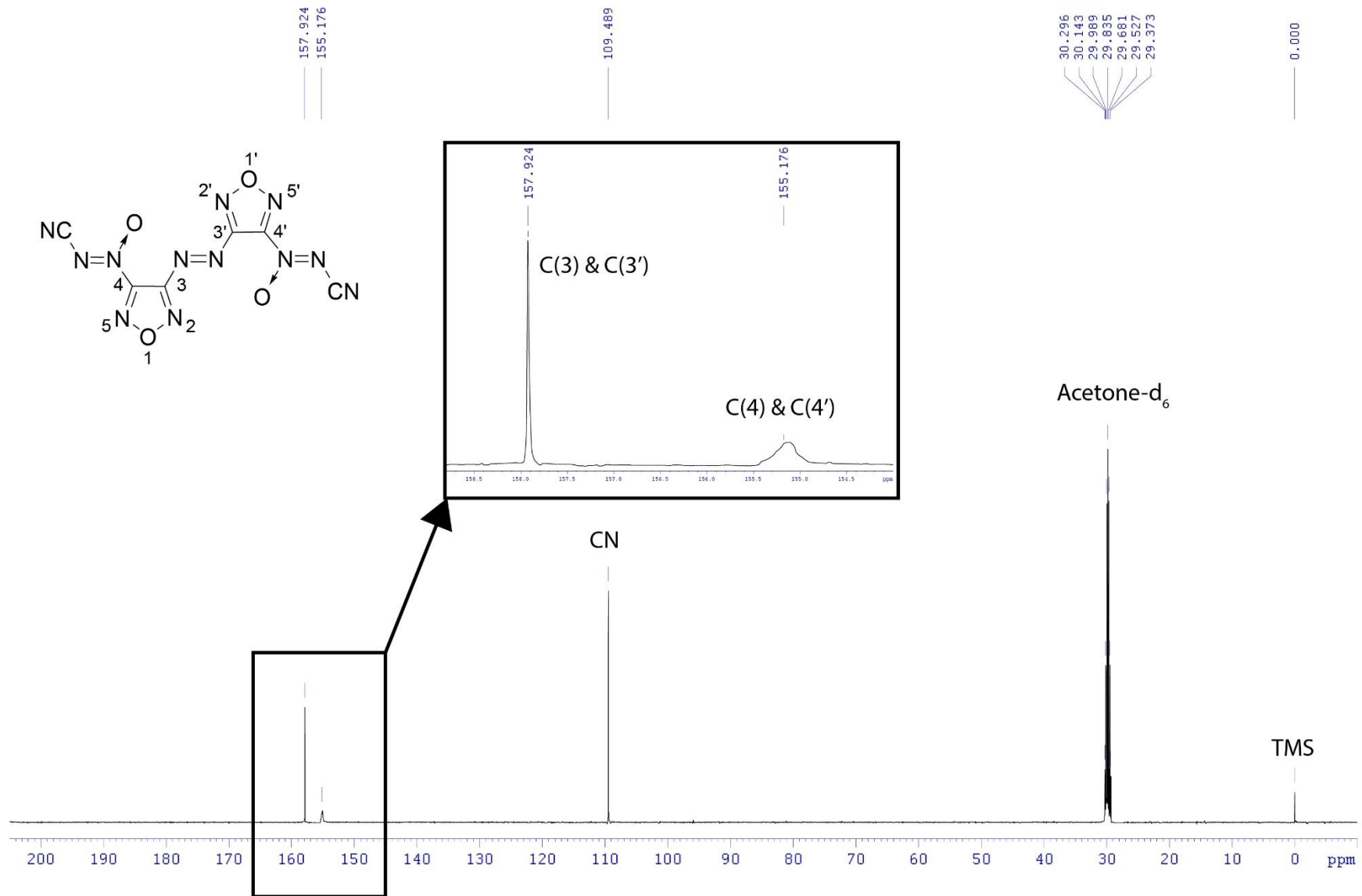
HRMS of compound 3

Acquisition Parameter

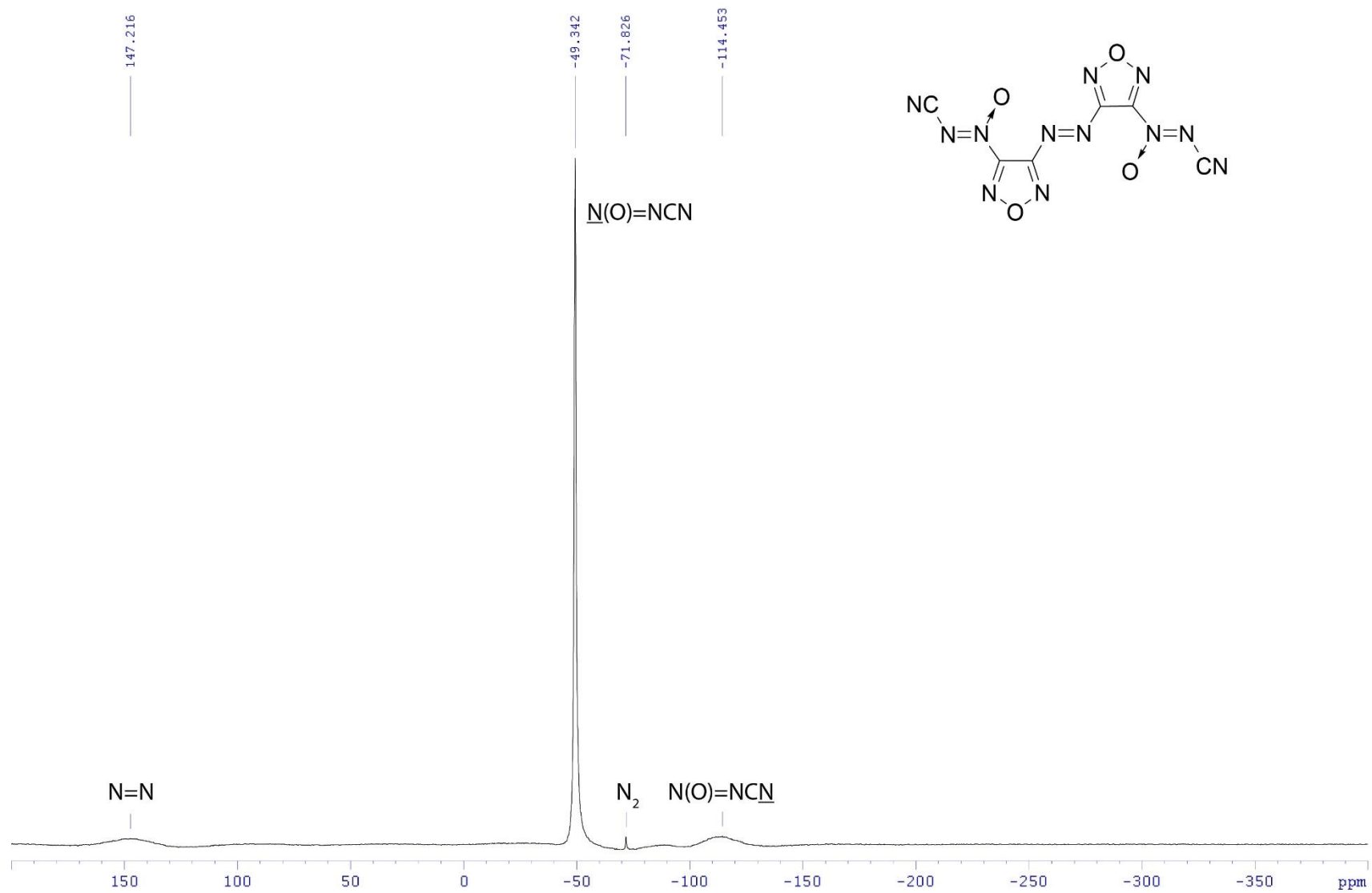
Source Type	ESI	Ion Polarity	Positive	Set Nebulizer	1.0 Bar
Focus	Not active			Set Dry Heater	200 °C
Scan Begin	50 m/z	Set Capillary	4500 V	Set Dry Gas	4.0 l/min
Scan End	1600 m/z	Set End Plate Offset	-500 V	Set Divert Valve	Waste



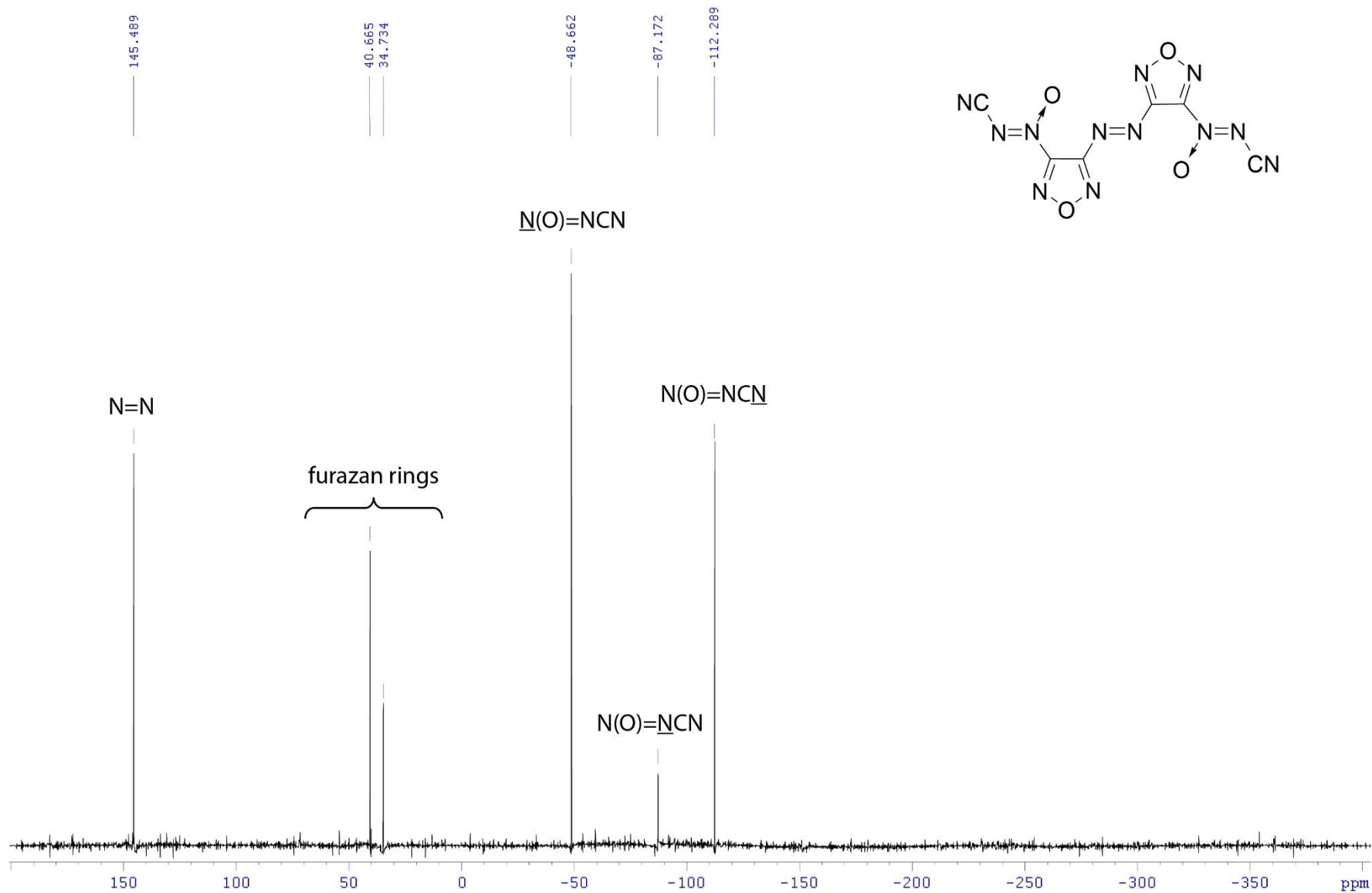
¹³C NMR (125.8 MHz, [D₆]acetone) spectrum of compound 4



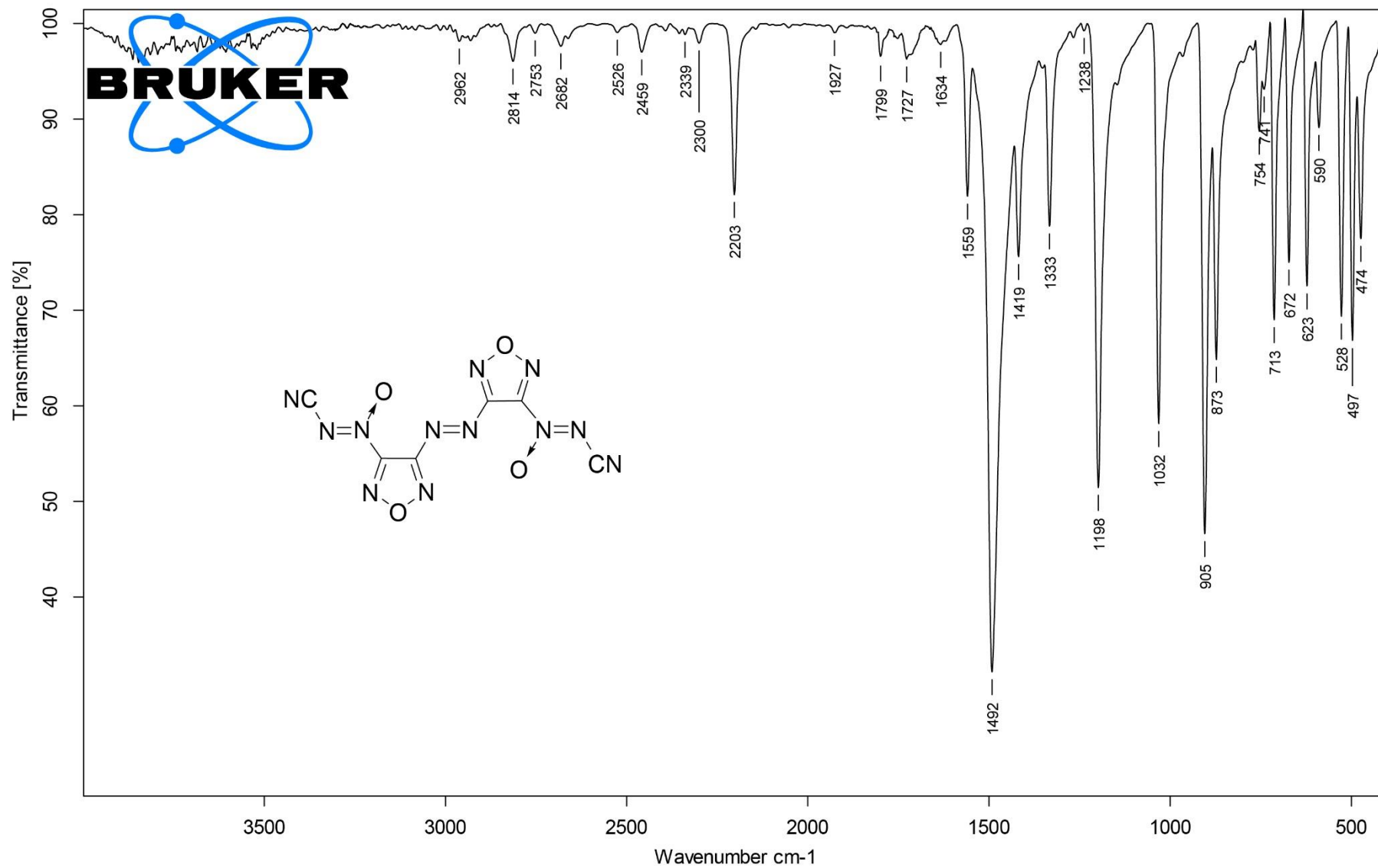
¹⁴N NMR (43.4 MHz, [D₆]acetone) spectrum of compound 4



^{15}N NMR ([INVGATED], 60.8 MHz, $[\text{D}_6]$ acetone) of compound 4



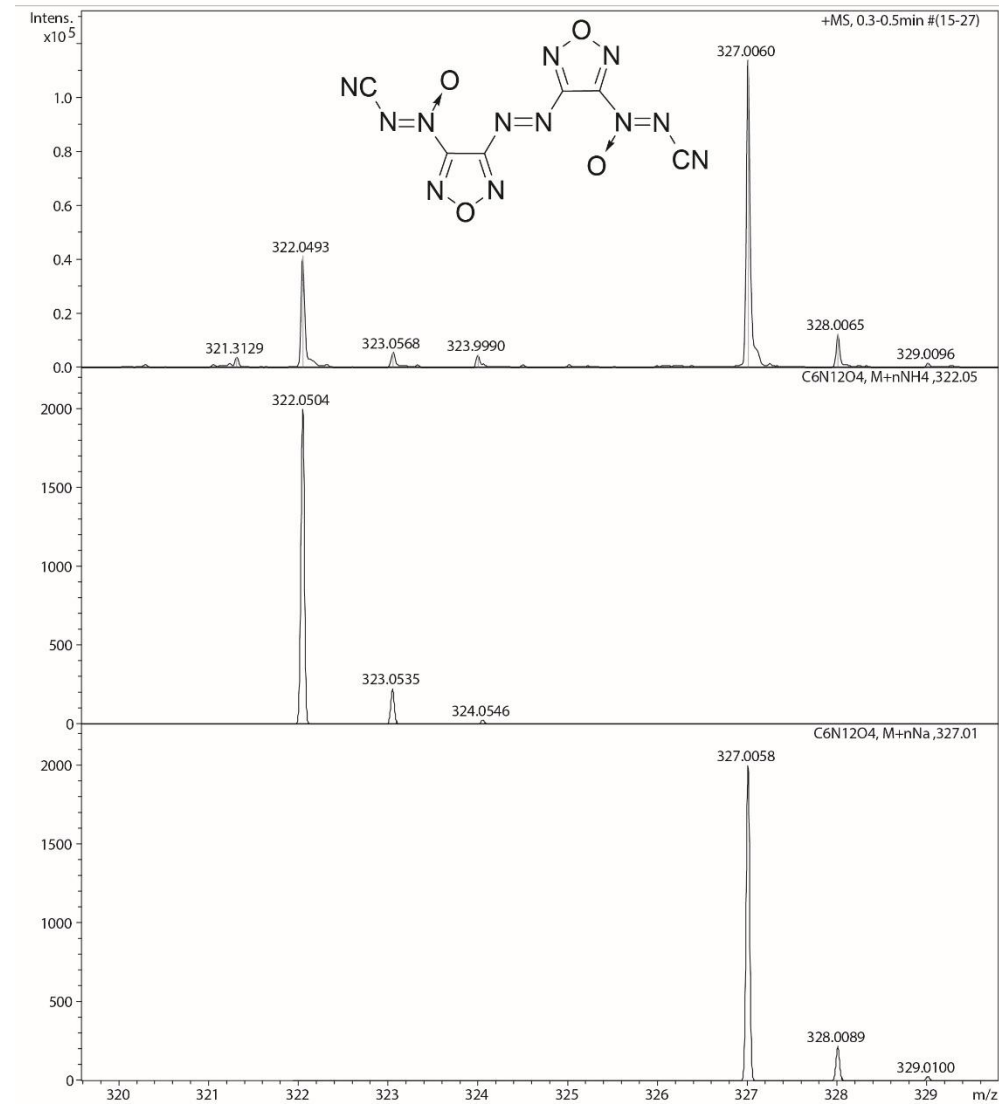
IR of compound 4



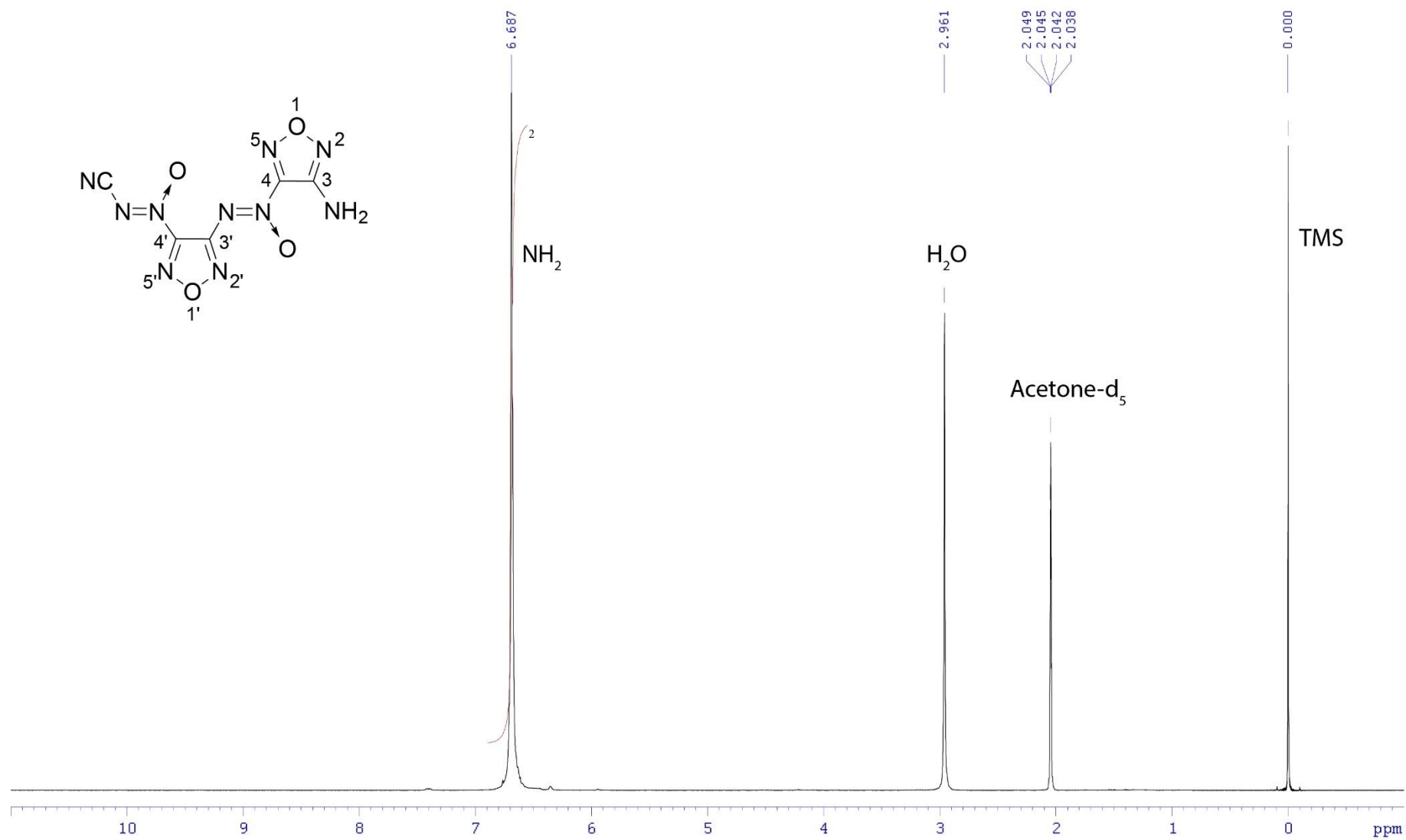
HRMS of compound 4

Acquisition Parameter

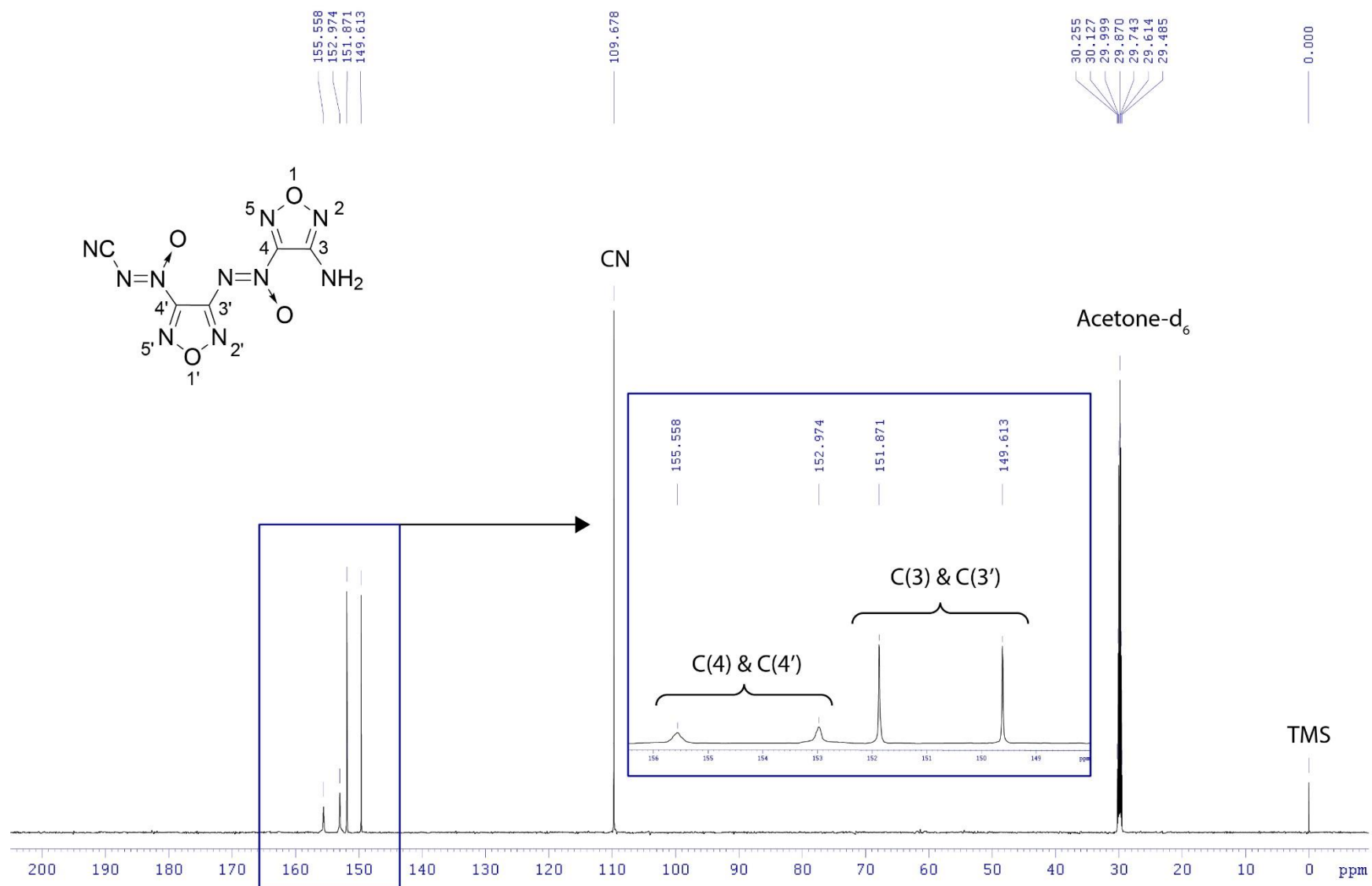
Source Type	ESI	Ion Polarity	Positive	Set Nebulizer	0.4 Bar
Focus	Not active			Set Dry Heater	180 C
Scan Begin	50 m/z	Set Capillary	4500 V	Set Dry Gas	4.0 l/min
Scan End	2500 m/z	Set End Plate Offset	-500 V	Set Divert Valve	Waste



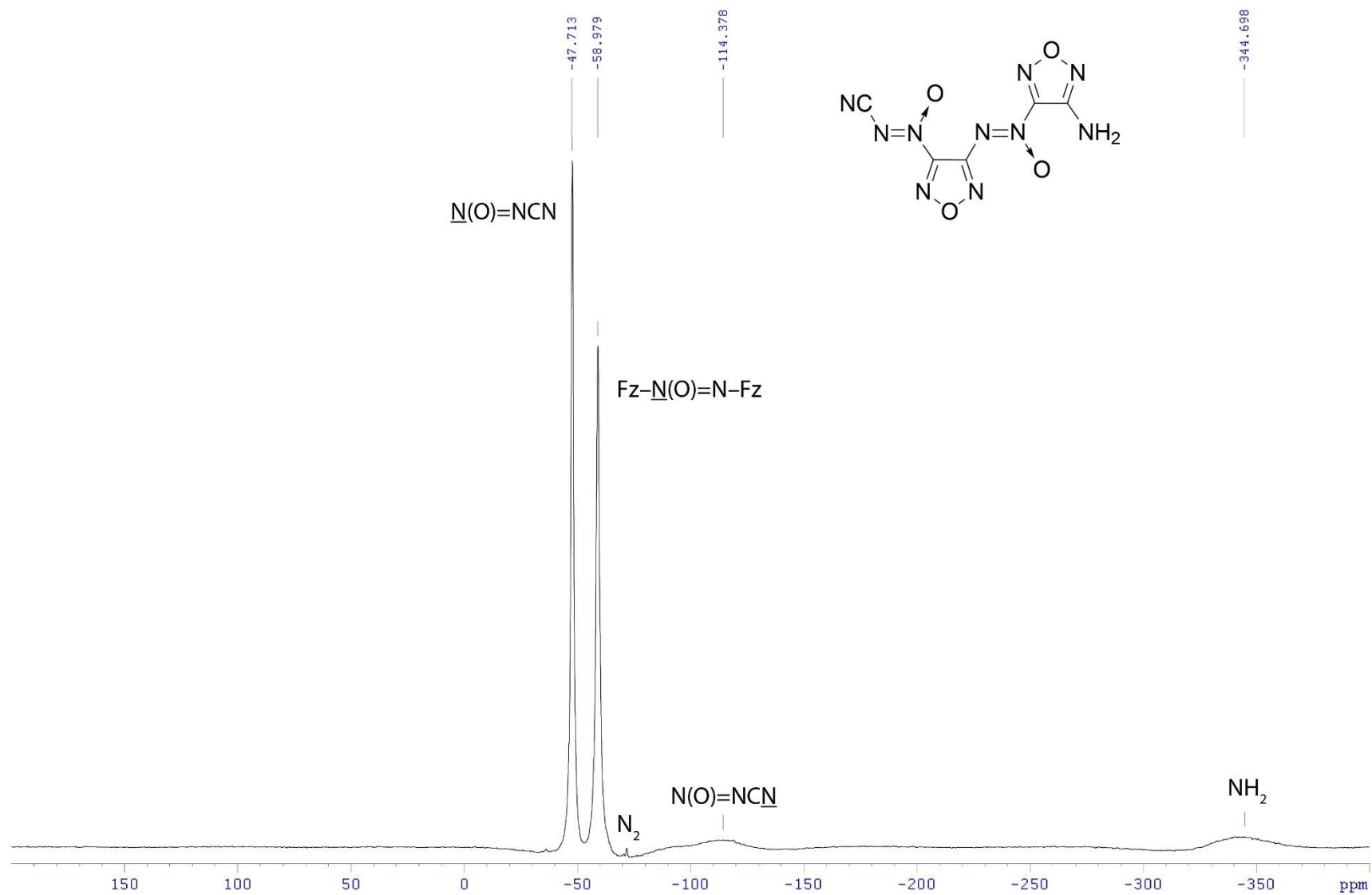
¹H NMR (600.1 MHz, [D₆]acetone) spectrum of compound 6



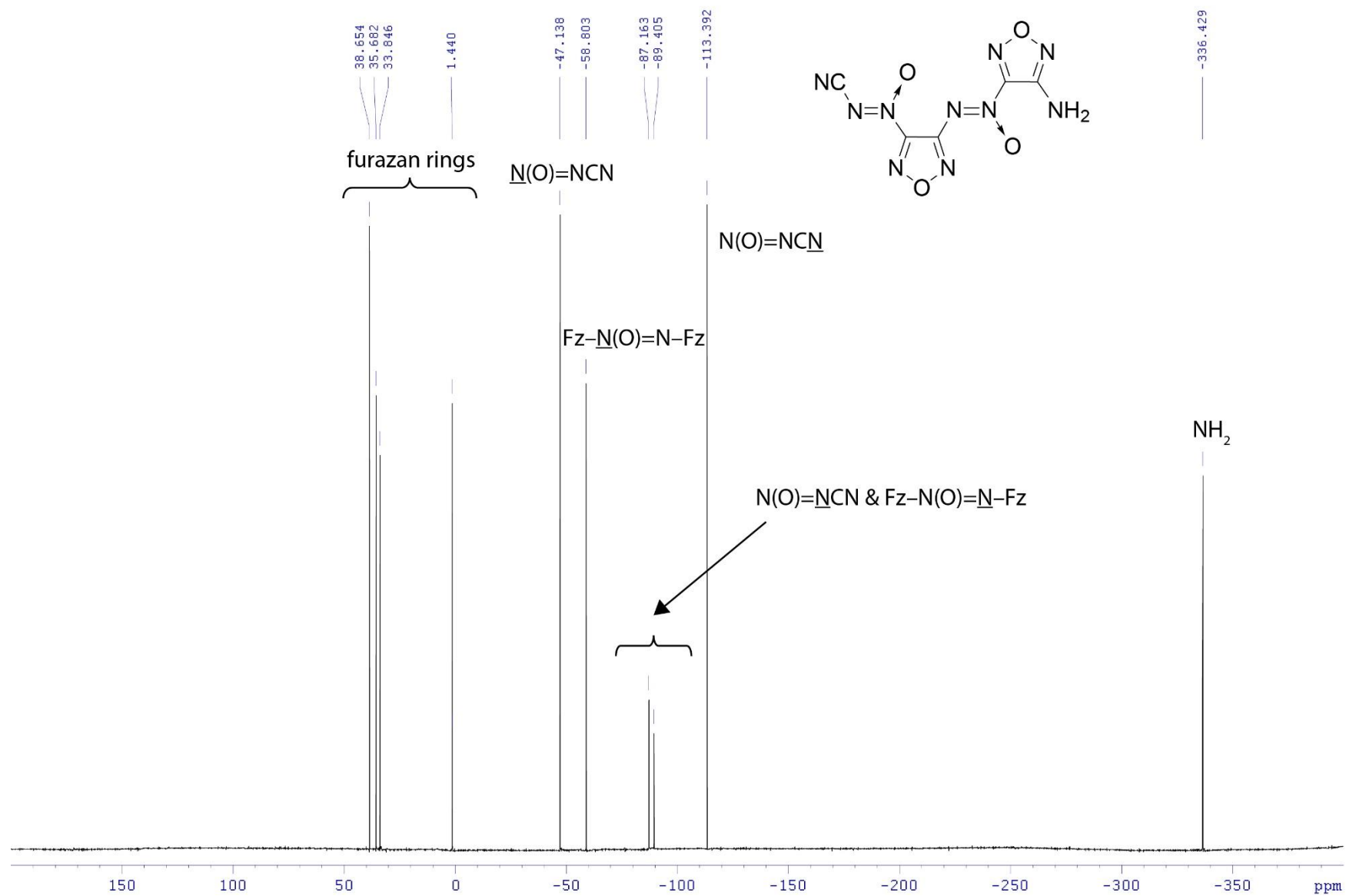
¹³C NMR (150.9 MHz, [D₆]acetone) spectrum of compound 6



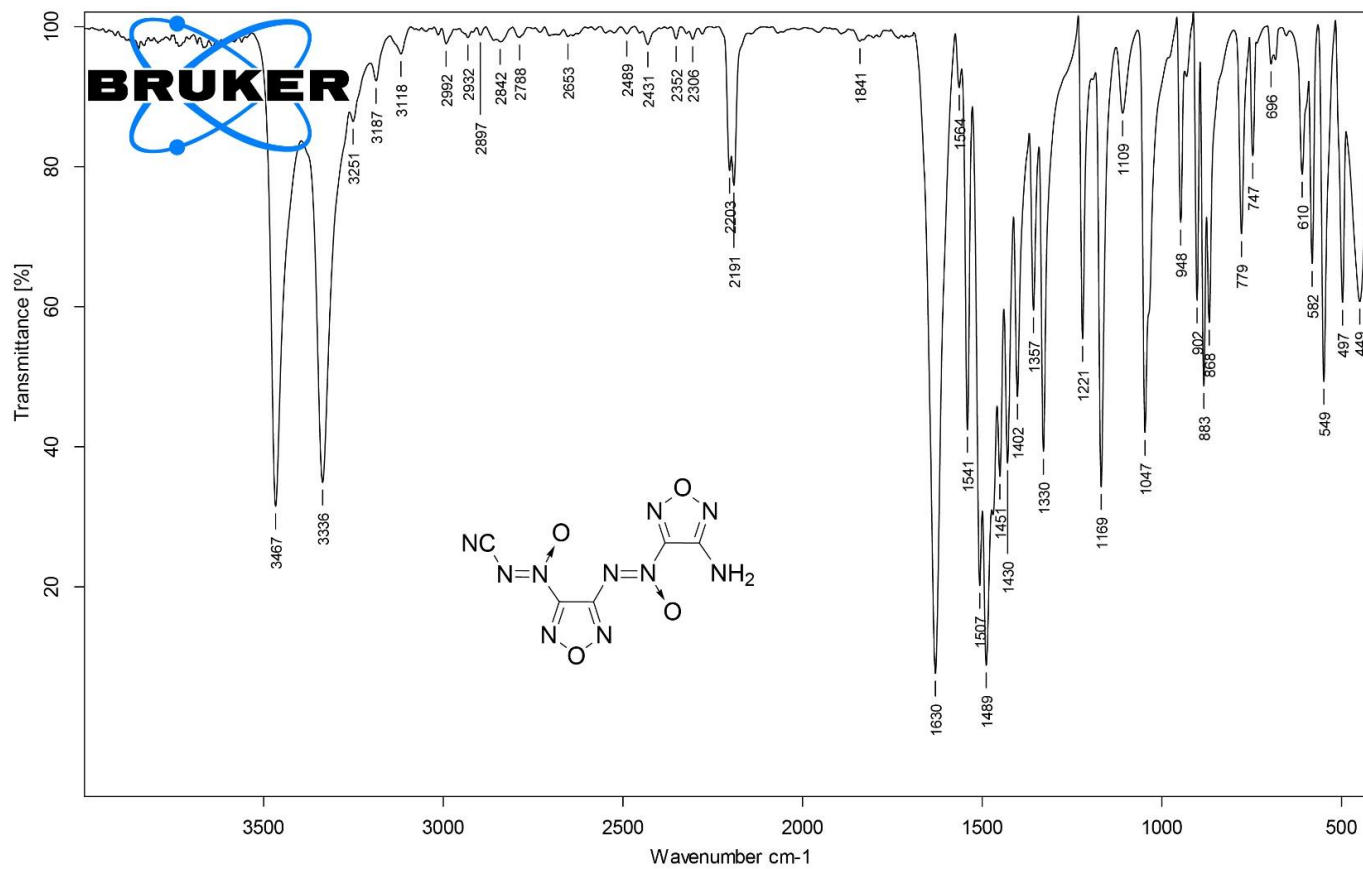
¹⁴N NMR (43.4 MHz, [D₆]acetone) of compound 6



¹⁵N NMR ([INVGATED], 60.8 MHz, [D₆]acetone) of compound 6



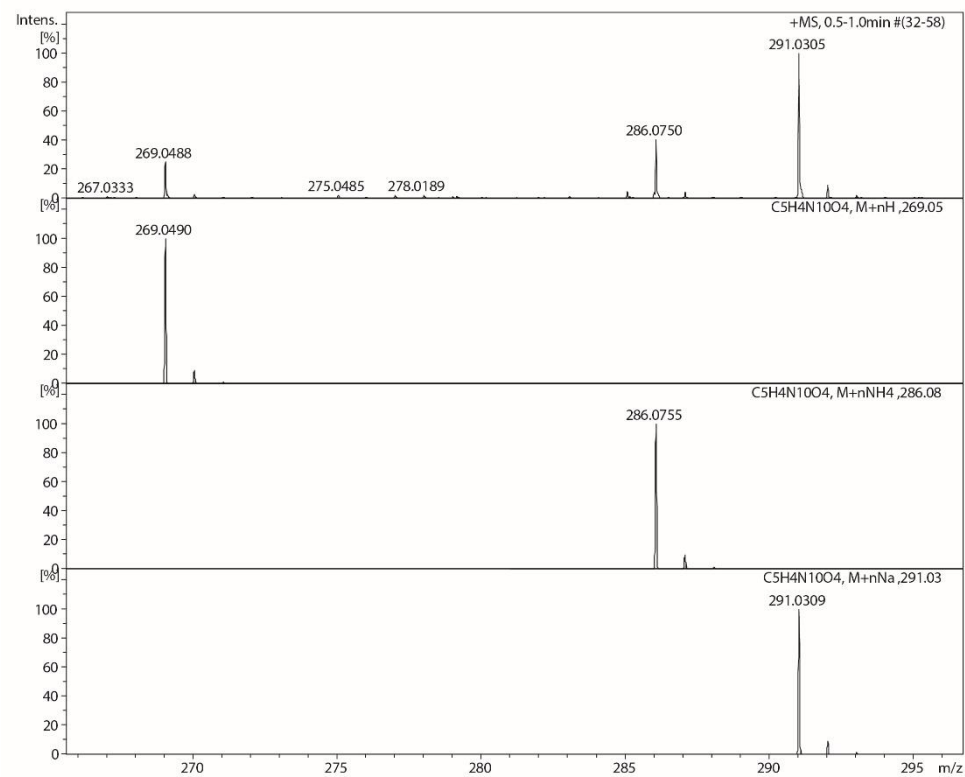
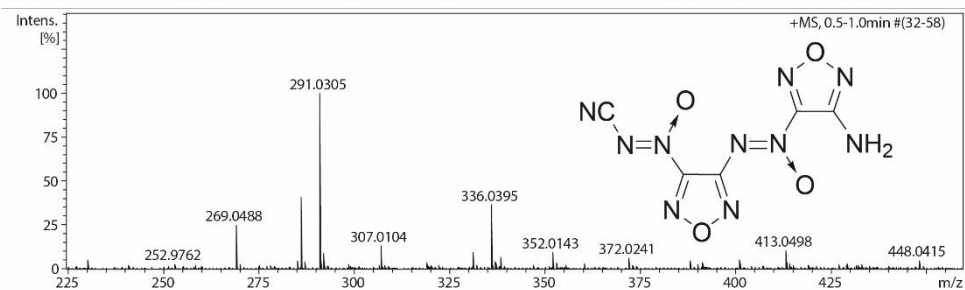
IR of compound 6



HRMS of compound 6

Acquisition Parameter

Source Type	ESI	Ion Polarity	Positive	Set Nebulizer	1.0 Bar
Focus	Not active			Set Dry Heater	200 °C
Scan Begin	50 m/z	Set Capillary	4500 V	Set Dry Gas	4.0 l/min
Scan End	1600 m/z	Set End Plate Offset	-500 V	Set Divert Valve	Waste



X-ray crystal structure determination

X-ray powder diffraction measurements were performed on a Bruker AXS D8 diffractometer (CuK α , $\lambda=1.534$ Å, reflection mode) equipped with a LynxEye position sensitive detector. Data collection was performed at ambient temperature with a step size of 0.02° and 1 s per step exposure for the 2θ range of 4–60°. Unit cell parameters for **3** and **4** were taken from low-temperature single-crystal experiments and refined with the Pawley method. For **6** powder diffraction pattern was indexed using the SVD (singular value decomposition) index algorithm⁴ as implemented in the Bruker TOPAS 5.0 software,⁵ the unit cell was further refined with the Pawley method, and the space group was determined using the analysis of systematic absences. Final unit cell data are provided in Table S1, and fits are shown in Figures S1–S3.

Table S1. Unit cell parameters and crystal density for compounds **3**, **4** and **6** determined by powder diffraction at room temperature (~298 K).

Compound	3	4	6
Space group	<i>Pnma</i>	<i>P2₁/n</i>	<i>P2₁/n</i>
Z / Z'	4 / 0.5	4 / 1	4 / 1
a, Å	12.7501(16)	8.7209(6)	10.6759(14)
b, Å	6.0210(7)	6.3422(5)	5.6105(8)
c, Å	7.8961(11)	11.3996(8)	16.872(2)
β , °		111.493(2)	93.683(4)
V, Å ³	606.17(13)	586.66(7)	1008.5(2)
<i>d</i> , g·cm ⁻¹	1.689	1.722	1.753

⁴ A. A. Coelho, *J. Appl. Crystallogr.*, 2003, **36**, 86.

⁵ A. A. Coelho, *J. Appl. Crystallogr.*, 2018, **51**, 210.

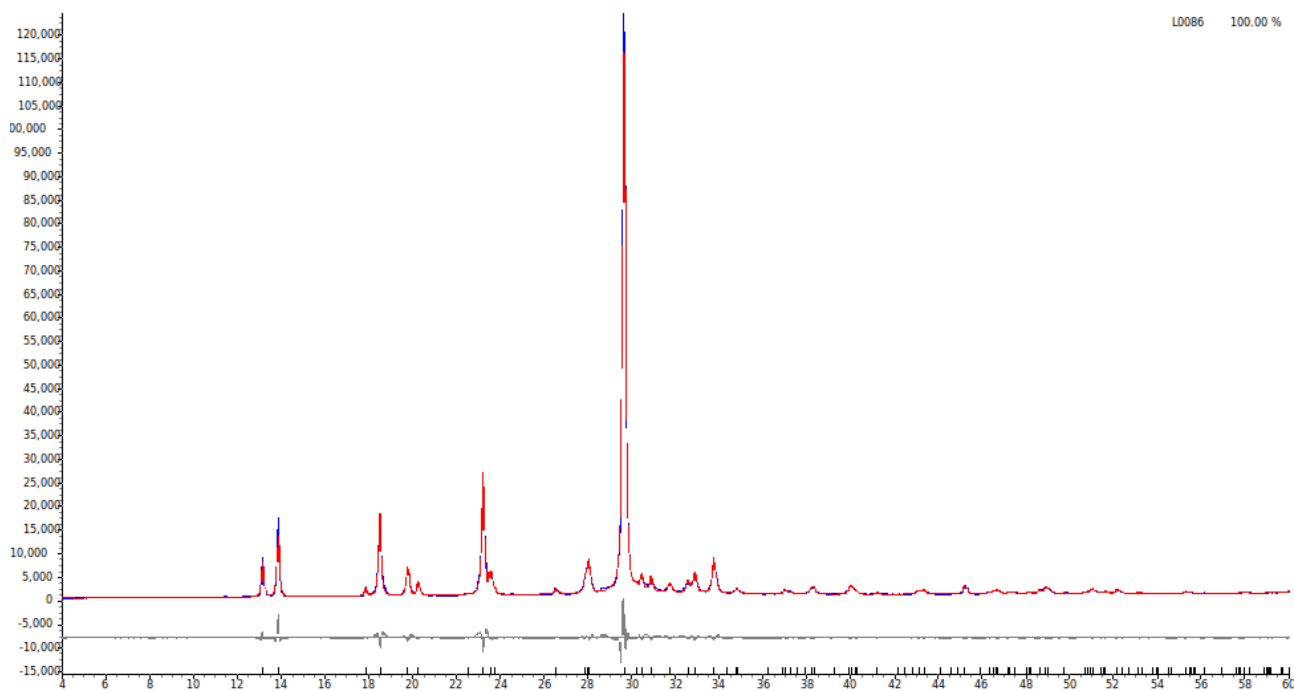


Figure S1. Pawley fit of PXRD data for aminofurazan **3** ($R_{wp} = 7.0$).

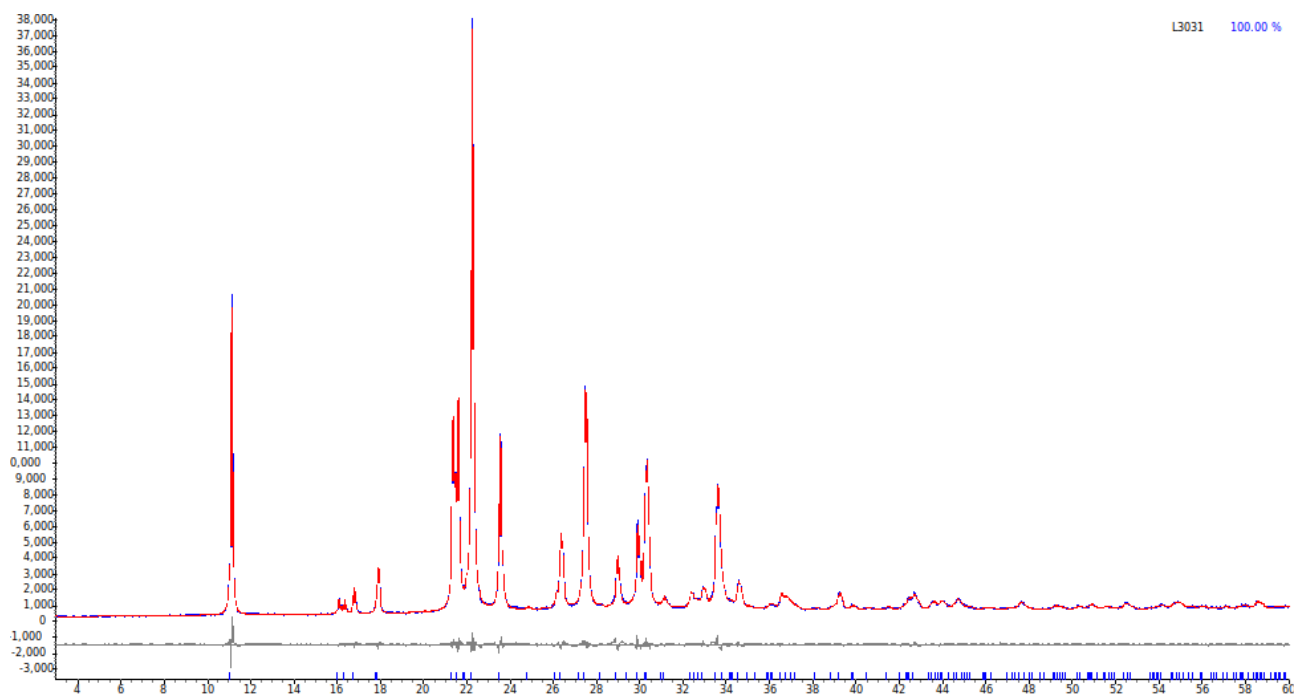


Figure S2. Pawley fit of PXRD data for azofurazan **4** ($R_{wp} = 4.6$).

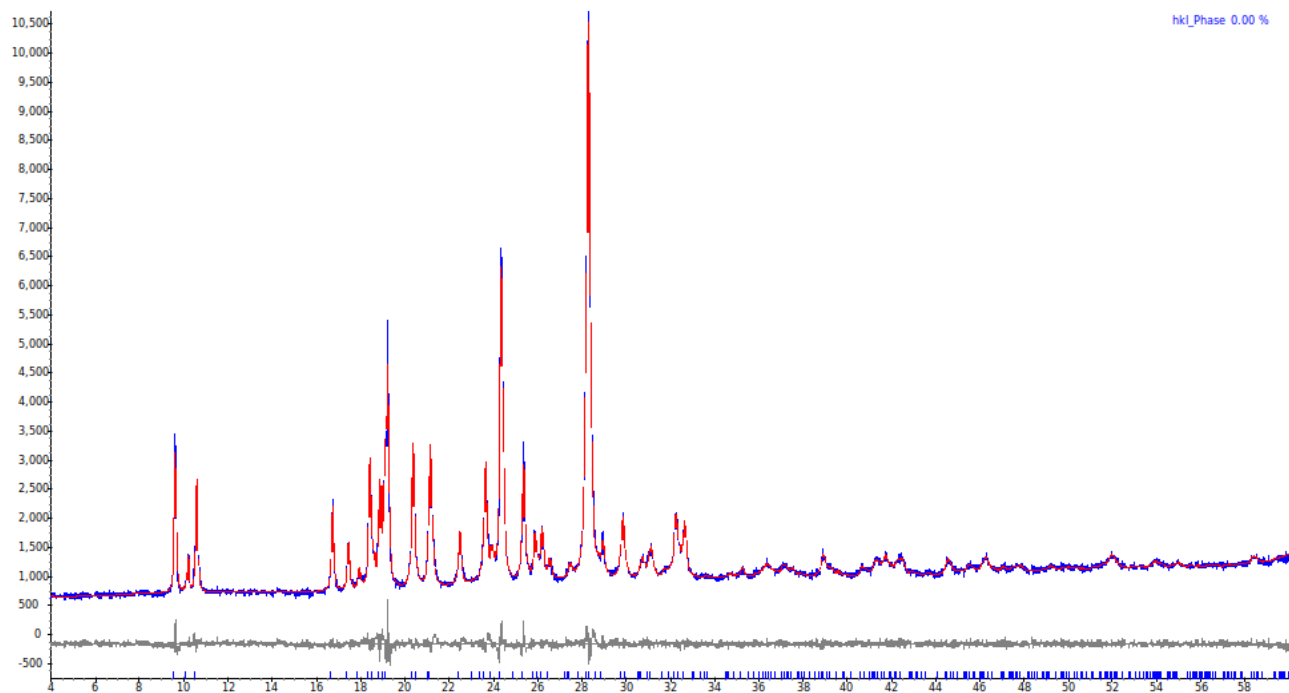


Figure S3. Pawley fit of PXRD data for azoxyfurazan **6** ($R_{wp} = 4.0$).

In crystal of (cyano-*NNO*-azoxy)furazan **3** one of the hydrogen atoms of the amino group H(6B) participate in intramolecular H-bond with the oxygen atom of cyano-*NNO*-azoxy fragment O(2) that favors the planar geometry of the molecule (N6···O2 2.8902(15) Å, N(6)–H(6B)···O2 121.0° with N–H set to 1.015 Å). In addition, weak intermolecular hydrogen bonds are formed with two neighboring molecules (Figure S4).

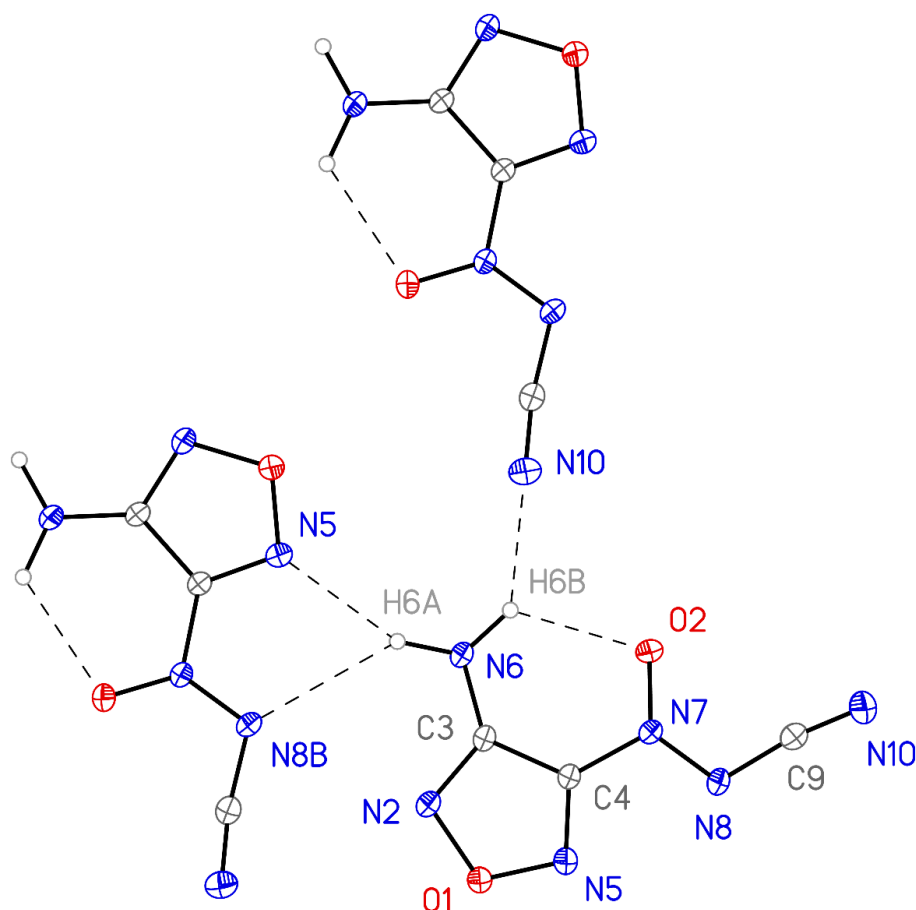


Figure S4. H-bonded associate in crystal of aminofurazan **3**. H-bond geometric parameters (N–H set to 1.015 Å): N(6)···O(2) 2.8902(15) Å, N(6)–H(6B)···O(2) 121.0°; N(6)···N(10) 2.9871(17) Å, N(6)–H(6B)···N(10) 138.7°; N(6)···N(5) 3.2064(16) Å, N(6)–H(6A)···N(5) 155.6°; N(6)···N(8) 3.450(18) Å, N(6)–H(6A)···N(8) 139.0°.

In crystal **6**·(CH₃)₂CO the cyano-*NNO*-azoxy fragment is disordered by two positions with very low occupancy of the second component (ca. 9%). In the latter structure intramolecular H-bonds are formed with nitrogen atom of the central azoxy fragment (N(6)···N(8) 2.8902(15) Å, N(6)–H(6B)···N(8) 116.6° with N–H set to 1.015 Å) and oxygen atom of the cyano-*NNO*-azoxy fragment connected to the other furazan ring (N(6)···O(3') 3.2934(15) Å, N(6)–H(6B)···O(3') 162.5°). The second hydrogen atom of the amino group connects molecules into centrosymmetric dimer via weak intermolecular H-bond (Figure S5). All

other intermolecular contacts in all crystals correspond to weak non-directional interactions.

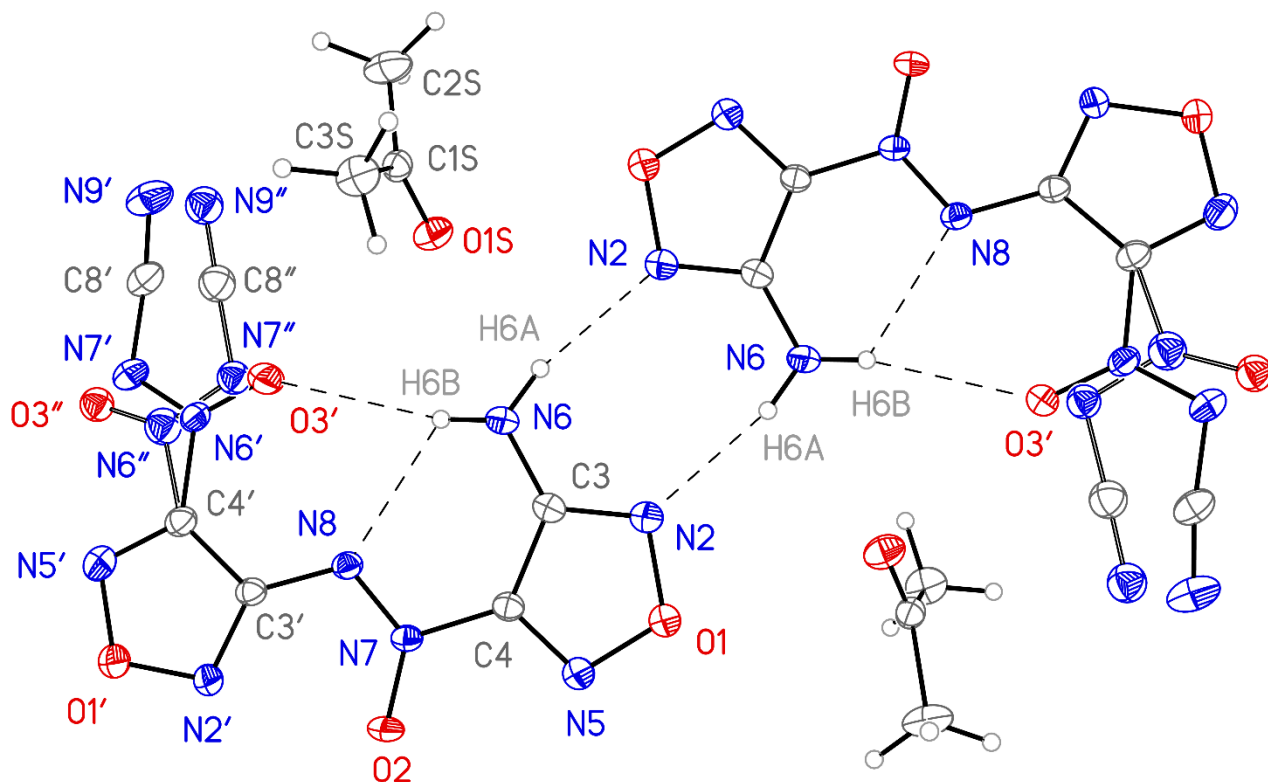
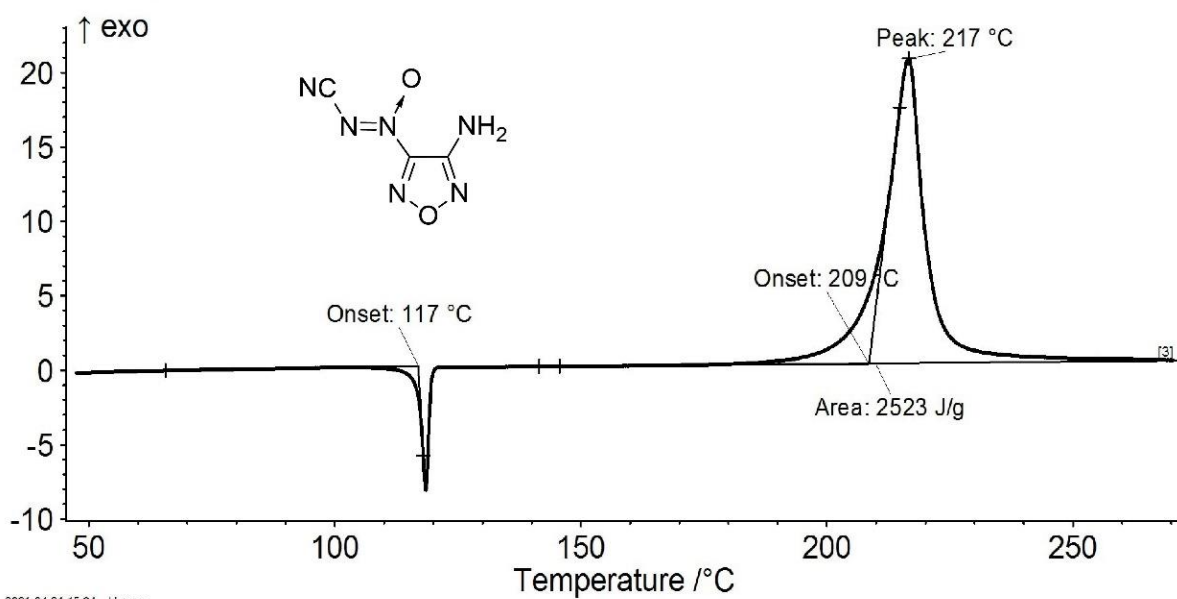


Figure S5. Centrosymmetric H-bonded dimer in crystal of azoxyfuran **6**. The H-bond geometric parameters (N–H set to 1.015 Å): N(6)⋯N(8) 2.8902(15) Å, N(6)–H(6B)⋯N(8) 116.6°; N(6)⋯O(3') 3.2934(15) Å, N(6)–H(6B)⋯O(3') 162.5°; N(6)⋯N(2) 3.1002(12) Å, N(6)–H(6A)⋯N(2) 163.3°. Solvate acetone molecules and the disorder of cyano-*NNO*-azoxy fragments (ca. 0.91:0.09) are also shown.

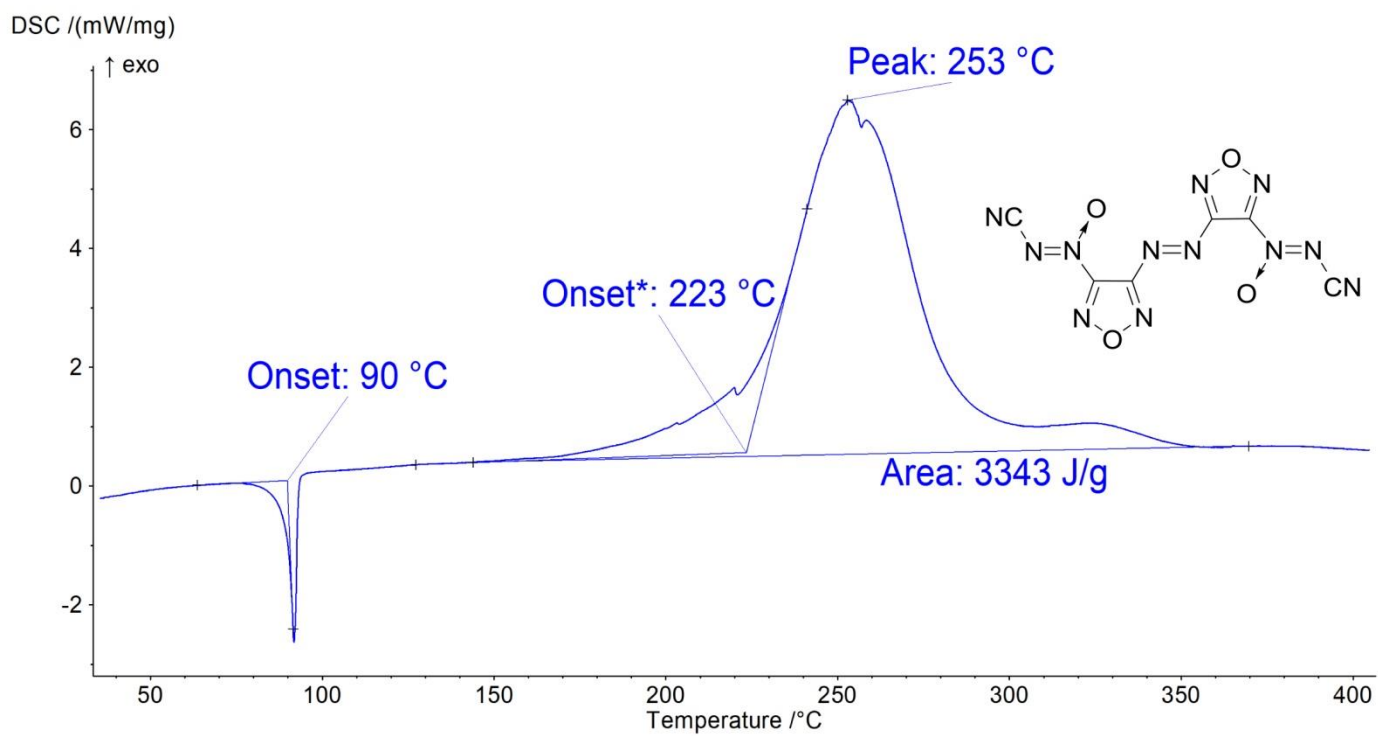
DSC of compound 3

DSC /(mW/mg)

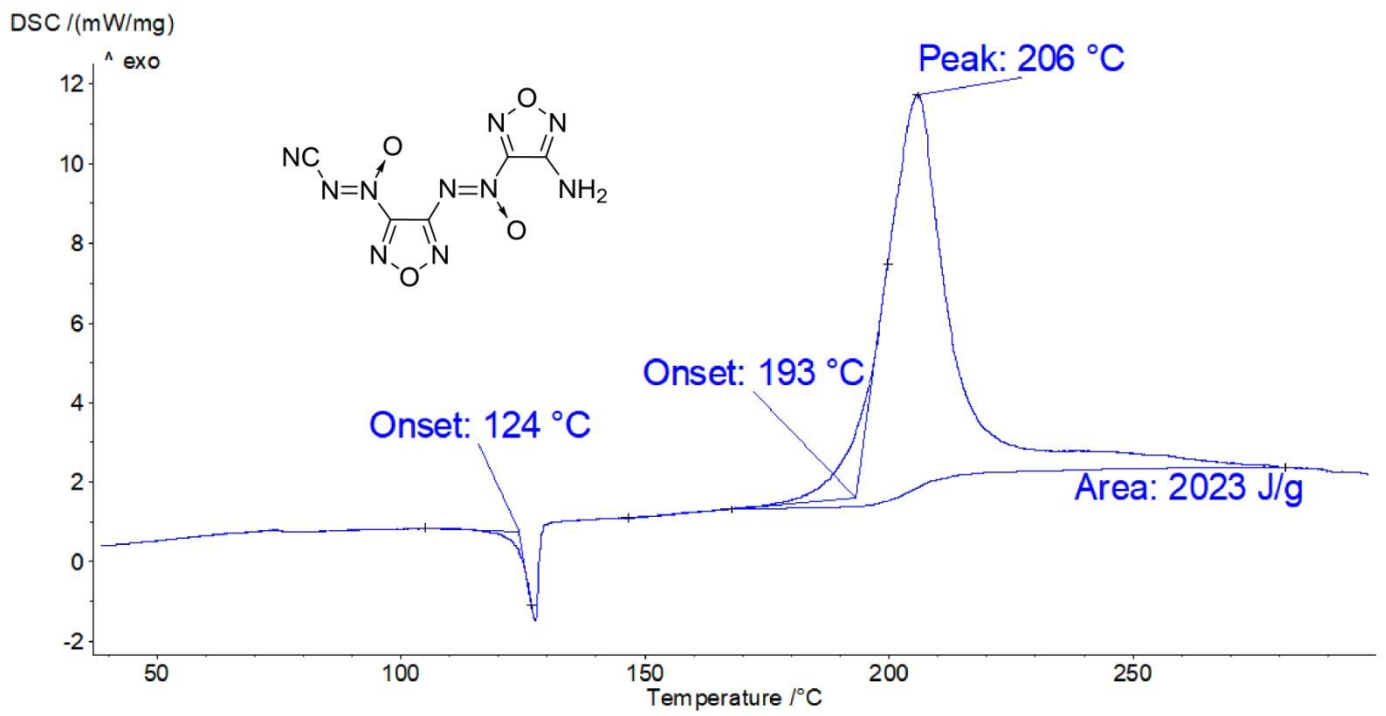


Main 2021-04-21 15:24 User: a

DSC of compound 4



DSC of compound 6



Calorimetric measurements

The main method for determining the enthalpy of formation of energetic compounds is combustion calorimetry. The measurements were performed on a precision automatic combustion calorimeter with an isothermal shell (designed by the Laboratory of Thermodynamics of High-Energy Systems of the Federal Research Center of Chemical Physics named after N. N. Semenov of the Russian Academy of Sciences for the combustion of energetic compounds).⁶

Basic design features of the calorimeter used in this study: 1) small heat equivalent ($\sim 500 \text{ cal} \cdot \text{degree}^{-1}$) with a large volume of bomb (200 cm^3); 2) simple installation bomb calorimeter – just remove the cap shell and the calorimetric vessel, drop the bomb and close the cover; 3) continuously thermostatic shell; 4) permanently fixed to the sheath liquid hermetic calorimeter vessel is in the form of a glass with double walls (calorimeter constant volume of fluid that delivers constant heat equivalent); 5) low measurement error. The calorimeter allows you to measure the thermal effect of the combustion reaction of substances with an extended uncertainty of 0.01–0.02%. Calibration of the calorimeter was carried out with the reference benzoic acid of the K-1 brand produced by the D. I. Mendeleev Institute of Metrology. The combustion energy of benzoic acid under standard conditions was $6322.6 \pm 1.2 \text{ cal} \cdot \text{g}^{-1}$. The absence of a systematic error in calorimetric measurements was controlled by burning secondary reference substances-succinic and hippuric acids, whose combustion energies on this calorimeter were $3020.3 \pm 0.6 \text{ cal} \cdot \text{g}^{-1}$ (0.02%) and $5631.4 \pm 3.4 \text{ cal} \cdot \text{g}^{-1}$ (0.06%), respectively. Samples of the studied substances **3**, **4** and **6** were burned in a platinum crucible. Pressed tablets of substances were weighed on Bunge microanalytic scales with an error of $2 \cdot 10^{-6} \text{ g}$. The suspended sample of the substance was placed in a calorimetric bomb and filled with oxygen. The initial oxygen pressure during the combustion of all substances is about 30 atm (3 MPa). Before the experiment, 1 mL of distilled water was injected into the bomb to create a saturated vapor pressure and dissolve the nitrogen oxides formed during the combustion process.

The samples were ignited with a cotton thread, which in turn was ignited by incandescent platinum wire (diameter 0.3 mm) with a dosed pulse of current supplied from a special device. The combustion energy of cotton yarn was measured in a series of seven experiments and amounted to $3968.9 \pm 1.6 \text{ cal} \cdot \text{g}^{-1}$. When determining the combustion energy, corrections for the thermal effects of nitric acid formation, heat exchange of a calorimetric vessel with an isothermal shell, and the combustion energy of the auxiliary substance and cotton thread were taken into account. A detailed procedure for preparing samples and conducting an incineration experiment was described earlier.⁷

⁶ Ya. O. Inozemtsev, A. B. Vorob'ev, A. V. Inozemtsev and Yu. N. Matyushin, *Combustion and Explosion (Gorenie i vzryv)*, 2014, **7**, 260.

⁷ T. S. Kon'kova, Yu. N. Matyushin, E. A. Miroshnichenko and A. B. Vorob'ev, *Russ. Chem. Bull.*, 2009, **58**, 2020.

The combustion energy ($-\Delta U'_B$, $\text{cal}\cdot\text{g}^{-1}$) under calorimetric bomb conditions for the studied compounds **3**, **4** and **6** is given in Tables TS2–TS4.

Table S2. Results of determination of the combustion energy of the compound **3**.

N	<i>m</i> , g	ΔT , °C	<i>Q</i> , cal	<i>q</i> _a , cal	<i>q</i> _i , cal	<i>q</i> _N , cal	<i>q</i> _{cot} , cal	$-U'_B$, $\text{cal}\cdot\text{g}^{-1}$
1	0.078181	2.14972	1155.67	900.47	7.18	2.48	8.34	3034.0
2	0.074154	2.12968	1144.89	902.48	7.26	2.21	7.77	3036.5
3	0.071614	2.11931	1139.32	904.25	7.24	2.14	8.18	3037.3
4	0.070382	2.10953	1134.06	902.97	7.26	2.10	8.11	3035.2
5	0.065308	2.10495	1131.60	1012.98	7.19	1.93	8.16	3034.1
$-\Delta U'_B = 3035.4 \pm 1.7 \text{ cal}\cdot\text{g}^{-1}$								

Table S3. Results of determination of the combustion energy of the compound **4**.

N	<i>m</i> , g	ΔT , °C	<i>Q</i> , cal	<i>q</i> _a , cal	<i>q</i> _i , cal	<i>q</i> _N , cal	<i>q</i> _{cot} , cal	$-U'_B$, $\text{cal}\cdot\text{g}^{-1}$
1	0.059938	2.16452	1163.62	969.85	7.20	2.21	7.74	2946.8
2	0.078976	2.16269	1162.64	910.78	7.38	2.97	8.34	2953.7
3	0.079116	2.22658	1196.99	945.72	7.22	2.88	7.98	2947.4
4	0.076468	2.22727	1197.36	954.04	7.20	2.79	7.88	2948.3
5	0.081933	2.09857	1128.17	869.29	7.18	2.62	7.70	2946.1
$-\Delta U'_B = 2948.5 \pm 3.5 \text{ cal}\cdot\text{g}^{-1}$								

Table S4. Results of determination of the combustion energy of the compound **6**.

N	m , g	ΔT , °C	Q , cal	q_a , cal	q_i , cal	q_N , cal	q_{cot} , cal	$-U'_B$, cal·g ⁻¹
1	0.079427	2.27970	1225.54	980.19	7.23	2.55	9.18	2850.3
2	0.079860	2.30055	1236.75	990.12	7.42	2.48	9.64	2842.7
3	0.077292	2.13244	1146.38	909.23	7.32	2.21	7.33	2850.1
4	0.075044	2.08133	1118.90	888.41	7.30	2.16	7.60	2844.1
5	0.070362	2.09606	1126.82	910.56	7.28	2.01	7.13	2840.2
$-\Delta U'_B = 2845.5 \pm 5.1 \text{ cal}\cdot\text{g}^{-1}$								

N – the ordinal number of the experiment;

m – weight of the sample of the compound in vacuum, g;

ΔT – corrected temperature rise in the calorimeter, degrees;

Q – the amount of heat measured in the experiment, cal;

q_a – heat of the combustion of the auxiliary substance benzoic acid, cal;

q_i – ignition energy, cal;

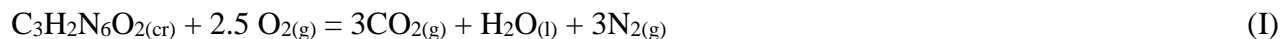
q_N – correction for the formation of nitric acid, cal;

q_{cot} – heat generation from combustion of the cotton thread, cal;

$\Delta U'_B$ – combustion energy of a substance in the bomb, cal·g⁻¹.

Calculation of the standard enthalpies of combustion and formation of the studied compounds 3, 4 and 6

The combustion reactions of compounds **3**, **4** and **6** proceed in accordance with the stoichiometry presented in equations (I) – (III), respectively:



where the indices "cr", "g" and "l" correspond to the crystalline, gaseous and liquid states, respectively, in this and subsequent equations.

The standard enthalpies of formation of substances **3**, **4** and **6** are calculated based on the enthalpies of combustion in accordance with equations (I) – (III):

$$\Delta H_f^\circ [\text{C}_3\text{H}_2\text{N}_6\text{O}_2]_{(\text{cr})} = 3\Delta H_f^\circ [\text{CO}_2]_{(\text{g})} + \Delta H_f^\circ [\text{H}_2\text{O}]_{(\text{l})} - \Delta H_c^\circ \quad (\text{IV})$$

$$\Delta H_f^\circ [\text{C}_6\text{N}_{12}\text{O}_4]_{(\text{cr})} = 6\Delta H_f^\circ [\text{CO}_2]_{(\text{g})} - \Delta H_c^\circ \quad (\text{V})$$

$$\Delta H_f^\circ [\text{C}_5\text{H}_2\text{N}_{10}\text{O}_4]_{(\text{cr})} = 5\Delta H_f^\circ [\text{CO}_2]_{(\text{g})} + \Delta H_f^\circ [\text{H}_2\text{O}]_{(\text{l})} - \Delta H_c^\circ \quad (\text{VI}),$$

where ΔH_c° – the standard enthalpy of combustion of the corresponding compound, $\text{kcal}\cdot\text{mol}^{-1}$, and ΔH_f° – the standard enthalpy of its formation, $\text{kcal}\cdot\text{mol}^{-1}$.

When calculating the standard enthalpies of formation of the studied compounds **3**, **4** and **6**, the reference values of the enthalpies of formation of combustion products were used:

$$\Delta H_f^\circ [\text{CO}_2]_{(\text{g})} = -94.051 \pm 0.031 \text{ kcal}\cdot\text{mol}^{-1} \text{ and}$$

$$\Delta H_f^\circ [\text{H}_2\text{O}]_{(\text{l})} = -68.315 \pm 0.009 \text{ kcal}\cdot\text{mol}^{-1}.^8$$

⁸ J. D. Cox, D. D. Wagman and V. A. Medvedev Eds., *CODATA key values for thermodynamics. Final Report of the CODATA Task Group on Key Values for Thermodynamics*, New York, Washington, Philadelphia, London, 1989.

Table S5. Thermochemical characteristics in the standard state of compounds **3**, **4** and **6**

Compound	$-\Delta U'_B$ cal·g ⁻¹	ΔH_c° kcal·mol ⁻¹	ΔH_f° kcal·mol ⁻¹
3	3035.4 ± 1.7	-464.8 ± 0.3	114.3 ± 0.3
4	2948.5 ± 3.5	-890.7 ± 1.1	326.4 ± 1.1
6	2845.6 ± 5.1	-752.3 ± 1.4	213.7 ± 1.4

Combustion performance

Energy potential of (cyano-*NNO*-azoxy)furazans **3**, **4** and **6** as components of solid fuels for rocket ramjet engines

The efficiency of using (cyano-*NNO*-azoxy)furazans **3**, **4** and **6** as energetic fillers (dispersants) of fuels for ramjet engines (RE) has been studied. Several years ago, it was proposed to use high-enthalpy poly-nitrogen compounds as energetic dispersants of solid fuels for RE.^{9,10,11}

The energy efficiency of metal-free solid fuels for ramjet engines is quite close to the linear dependence on the value of so called lower (that is if combustion products of organic components are gaseous CO₂ and not condensed water vapors at 25 °C) volumetric heat of combustion $Q_{v(\text{low})}$.¹² But this energy potential cannot be realized practically on the basis of even high-calorie hydrocarbons (for example, synthetic isoprene rubber SKI-3), since it is impossible to overcome diffusion difficulties when transferring outboard air to the surface of solid fuel. Therefore, to implement the possibility of high-speed combustion of such fuels, relatively small amount of oxidizing agent, for example, ammonium perchlorate NH₄ClO₄ (AP), was added to the fuel, in an amount much less than is required for solid composite propellants which do not use outboard air.^{13,14}

This technique allows at the first to carry out the adiabatic process of partial oxidation of the fuel (akin to combustion, but with a small reaction depth) with no external air access which leads to gasification and dispersion of the entire fuel mixture. After that, the transformed gasified and dispersed mixture enters the afterburner, where everything is burned to CO₂ and water vapor in a hot air stream, thereby providing energy to the propulsion system.

Thus, it was possible to achieve high rates of combustion of solid fuels. However, since the total value of $Q_{v(\text{low})}$ is a sum of partial values of $Q_{v(\text{low})}$ for all fuel components, and for AP it is an order of magnitude lower ($Q_{v(\text{low})} = 3120 \text{ MJ}\cdot\text{litre}^{-1}$) than for hydrocarbons, this approach significantly reduces the energy potential of fuels. It was shown that replacing AP as dispersant with some high-enthalpy poly-nitrogen compounds (enthalpy of formation 3000 kJ·kg⁻¹ and higher, $Q_{v(\text{low})}$ above 23 MJ·litre⁻¹) for a fuel that is a mixture of rubber with a dispersant leads to an increase in the aircraft flight range up to 18%.¹²

It was also shown that for dispersants the optimal value of the oxidizer excess coefficient α should be in the range 0.2–0.35, and the enthalpy of formation of the dispersant, the higher, other things being equal,

⁹ D. B. Lempert, S. V. Chapyshev, A. I. Kazakov, N. A. Plishkin, A. V. Shikhovtsev and L. S. Yanovskii, *Combust., Explos. Shock Waves*, 2019, **55**, 23 (*Fizika goreniya i vzryva*, 2019, **55**, 27).

¹⁰ L. S. Yanovskii, D. B. Lempert, V. V. Raznoschikov and I. S. Aver'kov, *Russ. J. Appl. Chem.*, 2019, **92**, 367 (*Zh. Prikl. Khim.*, 2019, **92**, 322).

¹¹ A. I. Kazakov, D. B. Lempert, A. V. Nabatova, D. V. Dashko, V. V. Raznoschikov, L. S. Yanovskii and S. M. Aldoshin, *Russ. J. Appl. Chem.*, 2019, **92**, 1696 (*Zh. Prikl. Khim.*, 2019, **92**, 1651).

¹² M. E. Reznikov, *Aviatsionnyye topliva i smazochnyye materialy (aviatsionnaya khimotologiya)*, Voennoye izdatel'stvo, 2004, p. 323 (in Russian).

¹³ V. N. Aleksandrov, V. M. Bytskevich, V. K. Verkholomov, M. D. Gramenitskiy, N. P. Dulepov, V. A. Skibin, Ye. V. Surikov, V. Ya. Khil'kevich and L. S. Yanovskiy, *Integral'nyye pryamotokhnnyye vozdušno-reaktivnyye dvigateli na tverdykh toplivakh (Osnovy teorii rascheta)*, Akademkniga, 2006, p. 343 (in Russian).

¹⁴ B. Kalpakli, E. B. Acar, A. Ulas, *Combust. Flame*, 2017, **179**, 267.

the better.¹⁵ These requirements are a consequence of the fact that an increase in the coefficient α of a dispersant inevitably decreases its value $Q_{v(\text{low})}$. On the other hand, the higher the value of the enthalpy of formation of the dispersant, the less it has to be added to the formulation, since in order for the fuel (rubber + dispersant) to start a spontaneous thermal transformation process, it is necessary that the calculated temperature of this adiabatic process (T_{ad}) reaches approximately 1500 K. And since all poly-nitrogen dispersants have $Q_{v(\text{low})}$ significantly lower than hydrocarbon fuels, an excessive increase in the proportion of dispersant negatively affects the energy potential of the fuel.

Thus, the creation of an optimized solid fuel formulation for RE is a compromise between the desire to obtain the maximum possible (potentially!) flight range of the aircraft (in the first approximation linearly dependent on $Q_{v(\text{low})}$ of the fuel) and the possibility of realizing high-speed thermal transformation at the first stage in a gas generator without air access.

The new (cyano-*NNO*-azoxy)furazans **3**, **4** and **6** described in this article were considered as potential dispersants of metal-free fuels for ramjet engines in a binary composition with synthetic isoprene rubber SKI-3. HMX and compounds **L-40** and **L-43** were considered as dispersants for comparison (Figure S6, Table TS6). HMX is much more effective as a dispersant than AP, but it is significantly inferior to compounds **L-40** and **L-43**, which showed the highest energy potential among the more than 40 components studied.¹²

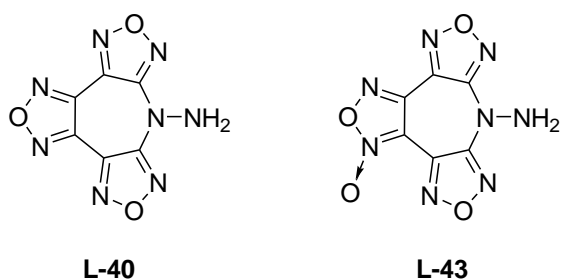


Figure S6. Structural formulas of compounds **L-40** and **L-43**.

¹⁵ D. B. Lempert, V. V. Raznoschikov and L. S. Yanovskii, *Russ. J. Appl. Chem.*, 2019, **92**, 1690 (*Zh. Prikl. Khim.*, 2019, **92**, 1578).

Table S6. Main characteristics of compounds considered as dispersants of solid fuels for ramjet engines

Compound	Gross formula	α^a	d^b , $\text{g}\cdot\text{cm}^{-3}$	$\Delta H_f^{\circ c}$, $\text{kJ}\cdot\text{kg}^{-1}$	T_{ad}^d , K	$Q_{u(\text{low})}^e$, $\text{MJ}\cdot\text{kg}^{-1}$	$Q_{v(\text{low})}^f$, $\text{MJ}\cdot\text{litr}^{-1}$
3	$\text{C}_3\text{H}_2\text{N}_6\text{O}_2$	0.29	1.69	+3106	2937	12.357	20.883
4	$\text{C}_6\text{N}_{12}\text{O}_4$	0.33	1.72	+4491	3962	12.263	21.093
6	$\text{C}_5\text{H}_2\text{N}_{10}\text{O}_4$	0.36	1.75	+3361	3489	11.678	19.853
HMX	$\text{C}_4\text{H}_8\text{N}_8\text{O}_8$	0.67	1.91 ^g	+255 ^g	3260	8.898	16.959
L-40	$\text{C}_6\text{H}_2\text{N}_8\text{O}_3$	0.23	1.85 ^h	+3090 ⁱ	2670	14.213	26.300
L-43	$\text{C}_6\text{H}_2\text{N}_8\text{O}_4$	0.31	1.88 ^j	+2805 ⁱ	3000	13.223	24.860
AP	NH_4ClO_4	2.0	1.95 ^g	-2517 ^g	1400	1.600	3.120

^a Oxidizer excess coefficient. For a compound with the molecular formula of $\text{C}_x\text{H}_y\text{N}_z\text{O}_z$, $\alpha = z/(2x + y/2)$.

^b Density. ^c Experimentally measured standard enthalpy of formation. ^d Temperature of adiabatic transformation of the substance in an individual state at 5 MPa calculated with the code TERRA. ^e Calculated lower specific heat of combustion. ^f Calculated lower volumetric heat of combustion

^g Ref.¹⁶ ^h Ref.¹⁷ ⁱ Ref.¹⁸ ^j Ref.¹⁹

For a correct comparison of the achieved values of $Q_{v(\text{low})}$, these values were compared for mixtures of dispersant + rubber SKI-3 at a ratio of these two components that ensured the achievement of T_{ad} of the mixture equal to 1500 K at a pressure of 5 MPa. The T_{ad} values were calculated using the TERRA code for calculating high-temperature chemical equilibria.²⁰

Table S7 and Figure S7 show the obtained data on the $Q_{v(\text{low})}$ values for the dispersant + SKI-3 rubber compositions at the component ratios corresponding to $T_{ad} = 1500$ K. It can be seen that the compositions with (cyano-*NNO*-azoxy)furazans **3**, **4** and **6** in terms of $Q_{v(\text{low})}$, they are significantly ahead of the compositions with HMX and AP. The composition with azofurazan **4** reaches practically the same $Q_{v(\text{low})}$ values as the compositions with the most effective high-enthalpy poly-nitrogen dispersants **L-40** and **L-43**.

¹⁶ R. Meyer, J. Kohler and A. Homburg, *Explosives*, 7th edn., Wiley-VCH, Weinheim, 2016.

¹⁷ A. I. Stepanov, D. V. Dashko and A. A. Astrat'yev, *Proizvodnyye 7H(7r)-tris[1,2,5]oksadiazolo-[3,4-*b*:3',4'-*d*:3'',4''-*f*]azepina i sposob ikh polucheniya*. Patent RU 2 534 989. 2014.

¹⁸ S. M. Aldoshin, D. B. Lempert, T. K. Goncharov, A. I. Kazakov, S. I. Soglasnova, E. M. Dorofeenko, N. A. Plishkin, *Russ. Chem. Bull. (Int. Ed.)*, 2016, **8**, 2018 (*Izv. Akad. Nauk, Ser. Khim.*, 2016, **8**, 2018).

¹⁹ H. Huo, J. Dong, B.-Z. Wang, Y.-S. Zhou, Z.-X. Ge and P. Lian, *Asian J. Chem.*, 2014, **26**, 7143.

²⁰ B. G. Trusov, "Program System TERRA for Simulation Phase and Thermal Chemical Equilibrium", XIV *Int. Symp. on Chemical Thermodynamics*, St-Petersburg, 2002, p. 483.

Table S7. $Q_{v(\text{low})}$ values for dispersant + SKI-3 rubber compositions at component ratios corresponding to $T_{\text{ad}} = 1500 \text{ K}$

Dispersant	$Q_{v(\text{low})}$ at $T_{\text{ad}} = 1500 \text{ K}$, $\text{MJ}\cdot\text{litre}^{-1}$	SKI-3 rubber content at T_{ad} $= 1500 \text{ K}$, w. %
AP	13.7	16.5
HMX	26.7	27.8
3	30.9	40.5
6	31.7	45.0
L-40	32.8	40.2
4	32.9	51.0
L-43	33.0	41.4

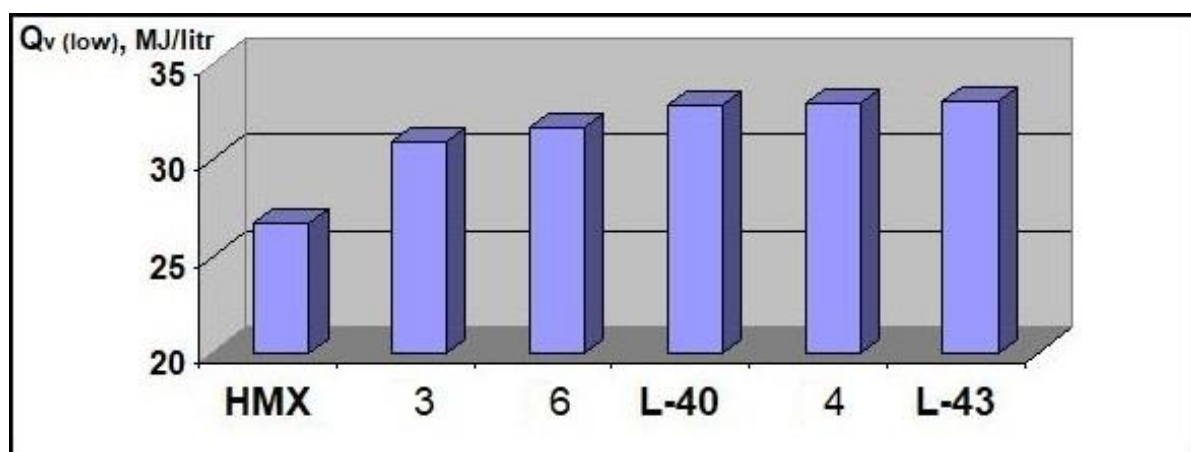


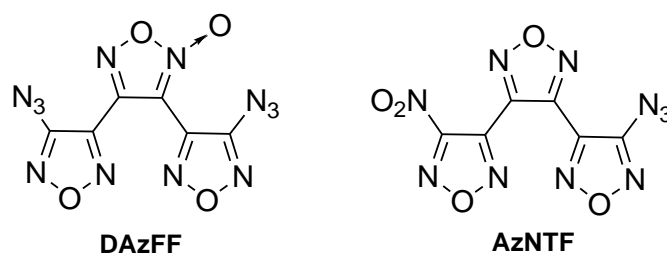
Figure S7. $Q_{v(\text{low})}$ values for dispersant + SKI-3 rubber formulations at component ratios corresponding to $T_{\text{ad}} = 1500 \text{ K}$.

Energy potential of (cyano-*NNO*-azoxy)furazans **3**, **4** and **6** as energetic fillers of solid composite propellants

The efficiency of using (cyano-*NNO*-azoxy)furazans **3**, **4** and **6** as energetic fillers of solid composite propellants (SCP) was studied. Compounds **3**, **4** and **6** have high values of the enthalpy of formation (from 3107 to 4490 kJ·kg⁻¹) and are characterized by a low oxygen content (oxidizer excess coefficient $\alpha = 0.29$ –0.36). Therefore, to compensate the deficiency of oxygen an additional oxidizing agent, ammonium perchlorate NH₄ClO₄ (AP), was introduced into the considered compositions in addition to the energetic fillers **3**, **4** and **6** as it was described earlier.^{21,22,23,24}

Such formulations of SCPs allow achieving sufficiently high values of specific impulse (I_{sp}) as applied to metal-free compositions, where the content of the main organic energetic filler is not very high (no more than 50 w.%, that ensures the safety of the manufacture and operation of the propellant).

SCP formulations were considered, consisting of three components: an energetic filler (compounds **3**, **4** and **6**, **HMX**, **RDX**, high-enthalpy furazans **DAzFF** ($\Delta H_f^\circ = 4291$ kJ·kg⁻¹, $d = 1.74$ g·cm⁻³; oxidizer excess coefficient $\alpha = 0.33$)²¹ and **AzNTF** ($\Delta H_f^\circ = 3279$ kJ·kg⁻¹, $d = 1.845$ g·cm⁻³; oxidizer excess coefficient $\alpha = 0.42$),²¹ oxidizer (ammonium perchlorate (**AP**)) and the active binder (C_{18.96}H_{34.64}N_{19.16}O_{29.32}, $\Delta H_f^\circ = -757$ kJ·kg⁻¹; $d = 1.49$ g·cm⁻³).²⁵



The ratio of the energetic filler and ammonium perchlorate in the formulations was varied at a constant volumetric content of the active binder of 19 vol.%. Note that at a lower volume fraction of the binder, it is difficult to safely manufacture the propellant mass, and at a higher volume fraction of the binder, the energy characteristics of the propellant, as a rule, decrease.

²¹ D. B. Lempert, A. I. Kazakov, V. S. Sannikov, A. V. Nabatova, D. V. Dashko and A. I. Stepanov, *Combust., Explos. Shock Waves*, 2019, **55**, 148 (*Fizika goreniya i vzryva*, 2019, **55**, 29).

²² D. B. Lempert, A. I. Kazakov, V. S. Sannikov, A. V. Nabatova, D. V. Dashko and A. I. Stepanov, *Combust., Explos. Shock Waves*, 2020, **56**, 301 (*Fizika goreniya i vzryva*, 2020, **56**, 6).

²³ I. Yu. Gudkova, I. N. Zyuzin, and D. B. Lempert. *Russ. J. Phys. Chem. B*, 2020, **14**, 302 (*Khimicheskaya fizika*, 2020, **39**, 53).

²⁴ I. N. Zyuzin, I. Yu. Gudkova, and D. B. Lempert. *Russ. J. Phys. Chem. B*, 2020, **14**, 804 (*Khimicheskaya fizika*, 2020, **39**, 52).

²⁵ D. Lempert, G. Nechiporenko and G. Manelis, *Cent. Eur. J. Energ. Mater.*, 2011, **8**, 25.

The specific impulse was calculated using the TERRA²⁰ standard code for calculating high-temperature chemical equilibria at pressures in the combustion chamber and at the nozzle exit of 4.0 and 0.1 MPa, respectively.

Table S8 shows the results of calculating specific impulses (I_{sp}) for the considered propellants formulations.

Table S8. Values of specific impulse (I_{sp}) and density (d) of compositions consisting of an energetic filler (compounds **3**, **4** and **6**, **HMX**, **RDX**, **DAzFF** and **AzNTF**), ammonium perchlorate (**AP**), and the active binder (19 vol.%, 15.4–17.1 w.%)

3 , w.%	AP , w.%	binder, w.%	d , g·cm ⁻³	I_{sp} , s
82.9	0	17.1	1.652	235.3
73.1	10	16.9	1.674	236.3
63.3	20	16.7	1.697	241.2
53.5	30	16.5	1.721	244.9
43.75	40	16.25	1.745	247.3
34	50	16	1.770	247.6
24.25	60	15.75	1.796	242.5
19.35	65	15.65	1.809	236.0
4 , w.%				
4 , w.%	AP , w.%	binder, w.%	d , g·cm ⁻³	I_{sp} , s
83.2	0	16.8	1.677	255.4
73.4	10	16.6	1.697	257.6
63.6	20	16.4	1.717	257.7
53.8	30	16.2	1.738	256.6
48.9	35	16.1	1.749	255.7
44	40	16	1.760	254.4
39.05	45	15.95	1.770	252.7
34.1	50	15.9	1.781	250.3
6 , w.%				
6 , w.%	AP , w.%	binder, w.%	d , g·cm ⁻³	I_{sp} , s
83.3	0	16.7	1.700	246.5
73.45	10	16.55	1.718	248.8
63.65	20	16.35	1.736	250.7
53.85	30	16.15	1.755	251.6
48.95	35	16.05	1.764	251.5
44.05	40	15.95	1.773	251.1
39.12	45	15.88	1.783	250.2
HMX , w.%				
HMX , w.%	AP , w.%	binder, w.%	d , g·cm ⁻³	I_{sp} , s
84.5	0	15.5	1.827	250.3
79.51	5	15.49	1.829	250.8
74.52	10	15.48	1.831	251.2
69.53	15	15.47	1.833	251.4
64.54	20	15.46	1.835	251.4
59.55	25	15.45	1.837	251.3
54.56	30	15.44	1.839	250.8
49.57	35	15.43	1.841	249.9
44.58	40	15.42	1.843	248.4
39.59	45	15.41	1.845	245.8

RDX, w.%	AP, w.%	binder, w.%	<i>d</i>, g·cm⁻³	<i>I</i>_{sp}, s
83.85	0	16.15	1.754	250.9
73.95	10	16.05	1.766	251.7
64.05	20	15.95	1.778	251.9
59.1	25	15.9	1.785	251.7
54.15	30	15.85	1.791	251.2
49.2	35	15.8	1.797	250.3
44.25	40	15.75	1.803	248.7
39.3	45	15.7	1.810	246.1
DAzFF, w.%				
DAzFF, w.%	AP, w.%	binder, w.%	<i>d</i>, g·cm⁻³	<i>I</i>_{sp}, s
73.5	10	16.5	1.713	253.1
68.55	15	16.45	1.722	254.9
58.7	25	16.3	1.741	255
53.8	30	16.2	1.751	254.7
48.9	35	16.1	1.76	254.1
43.95	40	16.05	1.769	253.0
39.05	45	15.95	1.779	251.5
AzNTE, w.%				
AzNTE, w.%	AP, w.%	binder, w.%	<i>d</i>, g·cm⁻³	<i>I</i>_{sp}, s
74.1	10	15.9	1.789	250.4
69.2	15	15.8	1.794	251
59.3	25	15.7	1.804	251.5
54.35	30	15.65	1.808	251.4
44.45	40	15.55	1.818	250.1
39.45	45	15.55	1.822	248.6

According to the calculations (see Table S8 and Figure S8), azofurazan **4** provides the highest values of specific impulse I_{sp} in comparison with all other considered energetic fillers with a content of 30–85 w.% in the propellant formulation. **DAzFF** compound is the second in terms of efficiency. Formulations based on azoxyfurazan **6**, with the energetic filler content above 55 w.%, are inferior in I_{sp} to similar formulations based on **HMX** and **RDX**, and with the energetic filler content below 55 w.% formulations with component **6** have higher I_{sp} than formulations based on standard components (**HMX**, **RDX**). The formulation containing aminofurazan **3** (40 w.%) has I_{sp} value close to the formulations containing **HMX** or **RDX** (40 w.%).

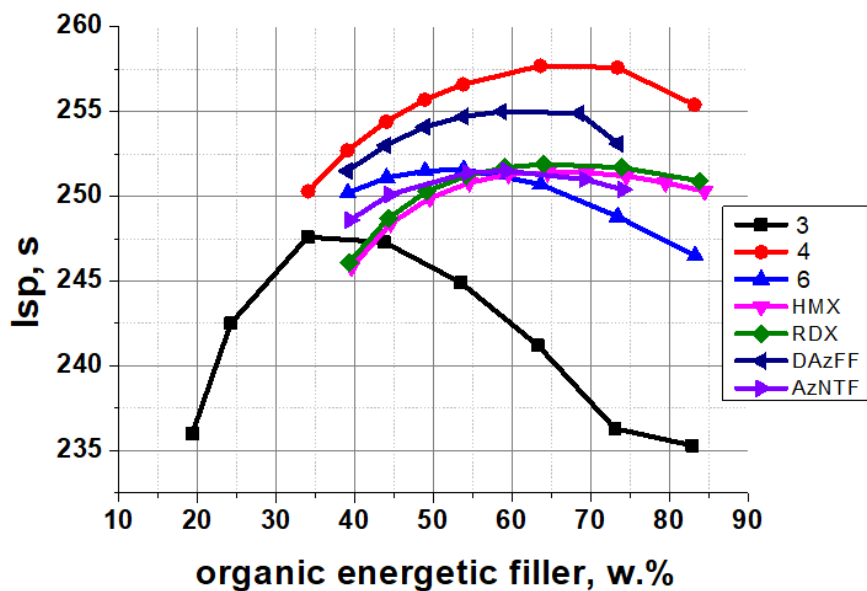


Figure S8. Formulations of the organic energetic filler + ammonium perchlorate (AP) + the active binder (19 vol.%, 15.4–17.1 w.%). Dependence of I_{sp} on the kind of the organic energetic filler and on the content of the latter in the formulation.

The values of specific impulses I_{sp} , achieved with the content of the considered energetic fillers in the SCP formulations in the amount of 40, 45 and 50 w.% are presented in the following histograms (Figures S9–S11).

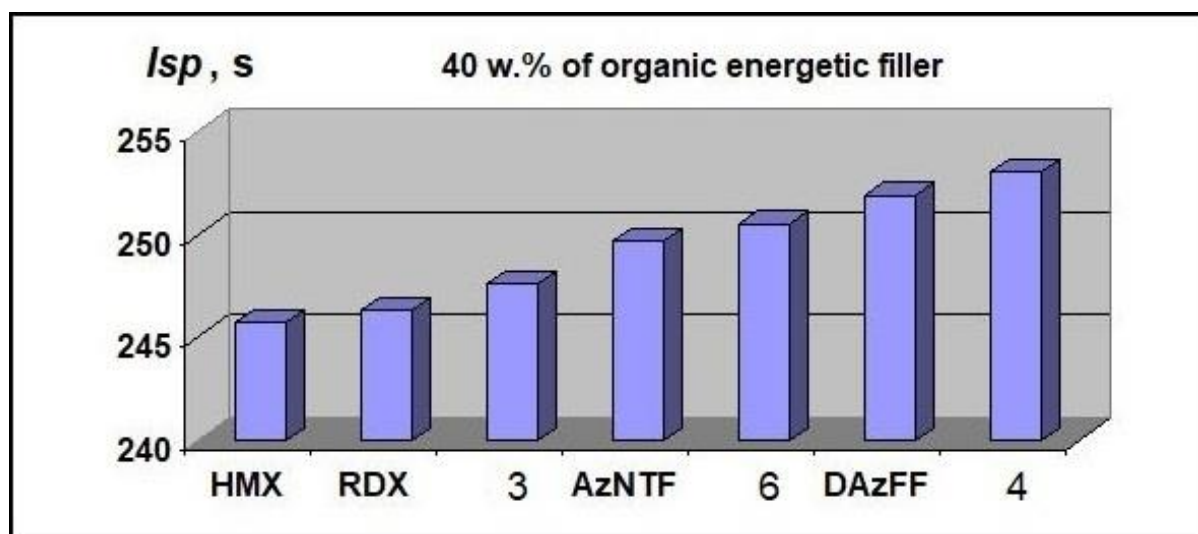


Figure S9. Formulations of the organic energetic filler (40 w.%) + ammonium perchlorate (AP) + the active binder (19 vol.%). Dependence of I_{sp} on the kind of the organic energetic filler.

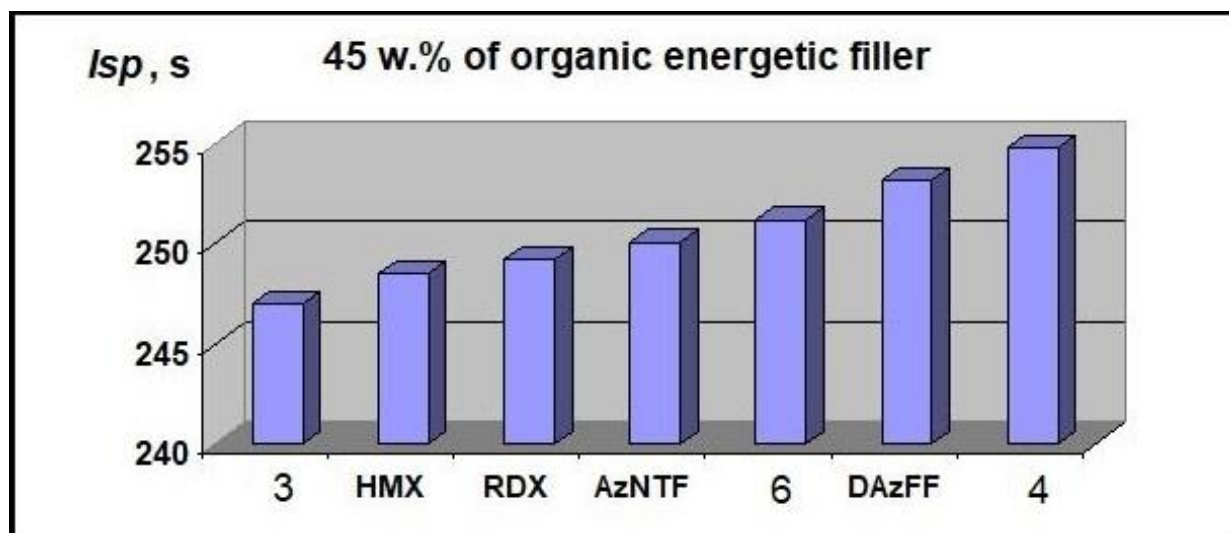


Figure S10. Formulations of the organic energetic filler (45 w.%) + ammonium perchlorate (AP) + the active binder (19 vol.%). Dependence of I_{sp} on the kind of the organic energetic filler.

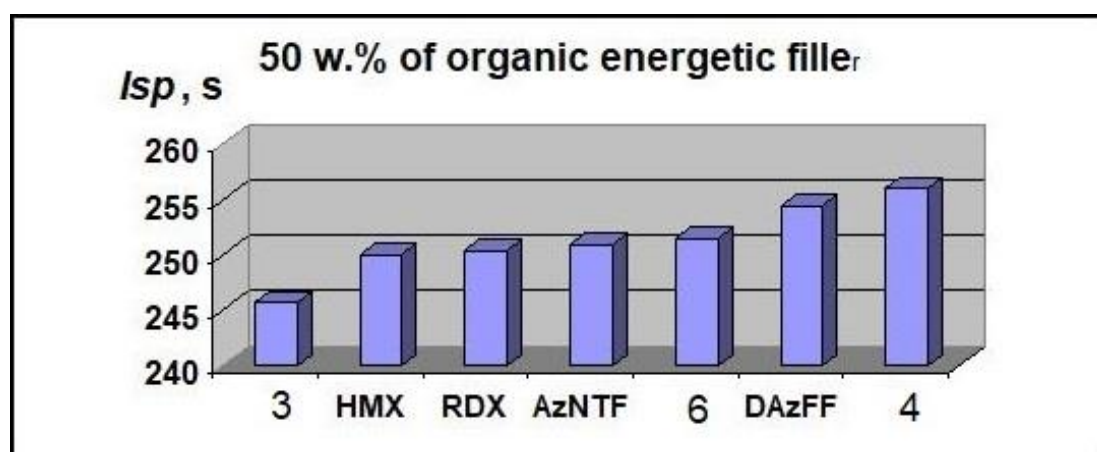


Figure S11. Formulations of the organic energetic filler (50 w.%) + ammonium perchlorate (AP) + the active binder (19 vol.%). Dependence of I_{sp} on the kind of the organic energetic filler.

Thus, the application of (cyano-*NNO*-azoxy)furazans **3**, **4** and **6** as energetic fillers of metal-free SCPs together with an additional oxidizer (ammonium perchlorate) makes it possible to create compositions with specific impulse $I_{sp} = 247\text{--}255$ s when the content of compounds **3**, **4** and **6** is not higher than 40–50 w.%, which allows safer manufacture and operation of propellants.